RESEARCH MEMORANDUM

WIND-TUNNEL INVESTIGATION AT TRANSONIC SPEEDS OF THE LIFT AND HINGE-MOMENT CHARACTERISTICS OF A FLAP WITH ATTACHED BALANCING TAB ON A 45° SWEPTBACK WING

By Raymond D. Vogler

Langley Aeronautical Laboratory
Langley Field, Va.

NATIONAL ADVISORY COMMITTEE
FOR AERONAUTICS

WASHINGTON

December 27, 1954

NATIONAL ADVISORY COMMITTEE FOR AERONAUTICS

RESEARCH MEMORANDUM

WIND-TUNNEL INVESTIGATION AT TRANSONIC SPEEDS OF THE LIFT AND HINGE-MOMENT CHARACTERISTICS OF A FLAP WITH ATTACHED BALANCING TAB ON A 45° SWEPTBACK WING

By Raymond D. Vogler

SUMMARY

An investigation was made at transonic speeds in the Langley high-speed 7- by 10-foot tunnel to determine the effect of an attached balancing tab on the lift and hinge-moment characteristics of a 25.4-percent-chord full-span flap on a tapered 45.6° sweptback wing with aspect ratio of 3 and thickness ratio of 0.076. The tab, located on the inboard trailing edge of the flap, had a chord and span one-half that of the flap. Lift and hinge-moment data were obtained for a range of tab deflection from 10° unbalancing to 30° balancing, flap deflections between ±20°, angles of attack from -2° to 16°, and a Mach number range from 0.75 to 1.20 obtained by using the transonic bump.

In order for the tab to balance the flap, a tab-flap deflection ratio of approximately 1 at subsonic speeds and 1.5 at supersonic speeds was indicated. The effectiveness of the balanced flap was about 80 percent of that of the unbalanced flap at zero angle of attack but decreased to about 67 percent at 16° angle of attack. At supersonic speeds, the rates of change of flap hinge moment with flap deflection, tab hinge moment with tab deflection, and tab hinge moment with flap deflection were approximately double the rates at subsonic speeds, but the rate of change of flap hinge moment with tab deflection varied less with Mach number than the aforementioned parameters.

INTRODUCTION

In the past few years the National Advisory Committee for Aeronautics has been studying the problem of balancing flap-type controls at transonic speeds by use of such devices as overhangs, horns, tabs, and auxiliary

surfaces. The results of some of these studies are reported in references 1 to 6. One method of balancing which has been successful at low speeds and, from the data of reference 3, appears promising at transonic speeds is the attached tab. At the present time, practically no tab hinge-moment data are available for the transonic speed range. It was the purpose of this investigation, therefore, to extend the Mach number range of tab and control hinge-moment data and, in addition, to determine the effect of an attached inboard tab on the lift effectiveness of a flap-type control on a swept wing.

This paper presents the results of an investigation of a low-aspect-ratio sweptback wing having a full-span flap with an attached inboard tab. The chord and span of the tab were one-half of the chord and span of the flap. Lift and hinge-moment data were obtained for a range of tab deflection generally from a 10° unbalancing deflection to a 30° balancing deflection, flap deflections between $\pm 20^\circ$, angles of attack from -2° to 16°, and a Mach number range from 0.75 to 1.20.

SYMBOLS AND COEFFICIENTS

C_L lift coefficient, $\dfrac{\text{Twice semispan lift}}{qS}$

C_{h_f} flap hinge-moment coefficient,

$$\frac{\text{Flap hinge moment about hinge line of flap}}{q2M'_f}$$

C_{h_t} tab hinge-moment coefficient,

$$\frac{\text{Tab hinge moment about hinge line of tab}}{q2M'_t}$$

ΔC_{h_f} increment of flap hinge-moment coefficient produced by flap deflection

q effective dynamic pressure, $\rho V^2/2$, lb/sq ft

S twice wing area of semispan model including tab, 0.216 sq ft

$\bar{c}$ mean aerodynamic chord (tab excluded), 0.268 ft

ρ mass density of air, slugs/cu ft

V free-stream air velocity, ft/sec

M'_f area moment of flap (including tab) behind hinge line about hinge line for semispan wing, 0.00122 ft^3

M'_t area moment of tab behind hinge line about hinge line for semispan wing, 0.000111 ft^3

M effective Mach number

M_l local Mach number

R Reynolds number based on mean aerodynamic chord

α angle of attack, deg

δ_f flap deflection, angle between wing-chord plane and flap-chord plane measured in a plane perpendicular to flap hinge line; positive when trailing edge of flap is down, deg

δ_t tab deflection, angle between flap-chord plane and tab-chord plane measured in a plane perpendicular to tab hinge line; positive when trailing edge of tab is down, deg

$$C_{h_{t_{\delta_t}}} = \left(\frac{\partial C_{h_t}}{\partial \delta_t}\right)_{\alpha,M,\delta_f=0}$$

$$C_{h_{t_{\delta_f}}} = \left(\frac{\partial C_{h_t}}{\partial \delta_f}\right)_{\alpha,M,\delta_t=0}$$

$$C_{h_{f_{\delta_f}}} = \left(\frac{\partial C_{h_f}}{\partial \delta_f}\right)_{\alpha,M,\delta_t=0}$$

$$C_{h_{f_{\delta_t}}} = \left(\frac{\partial C_{h_f}}{\partial \delta_t}\right)_{\alpha,M,\delta_f=0}$$

$$C_{L_{\delta_f}} = \left(\frac{\partial C_L}{\partial \delta_f}\right)_{\alpha,M,\delta_t=0}$$

$$C_{l_{\delta_t}} = \left(\frac{\partial C_l}{\partial \delta_t}\right)_{\alpha,M,\delta_f=0}$$

$$\left(C_{l_{\delta_f}}\right)_{\Delta C_{h_f}=0} = C_{l_{\delta_f}} - \frac{\delta_t}{\delta_f} C_{l_{\delta_t}}$$

where

$$\frac{\delta_t}{\delta_f} = \frac{C_{h_{f_{\delta_f}}}}{C_{h_{f_{\delta_t}}}}$$

Subscripts outside parentheses indicate factors held constant during measurement of parameters.

MODEL AND APPARATUS

The steel semispan basic wing (excluding tab) model used in the investigation had a quarter-chord sweep angle of 45.6°, an aspect ratio of 3, a taper ratio of 0.5, and a thickness ratio of approximately 7.6 percent based on the streamwise chord (fig. 1). The airfoil section measured in a plane at 45° to the plane of symmetry was an NACA 64A010 except for the inboard 50 percent span back of the flap hinge line. Over the span of the flap occupied by the tab, the flap had been altered in profile by fairing a straight line from the flap hinge line to the trailing edge of the tab. Beyond this region, the normal airfoil sections were used as shown in figure 1. The wing was equipped with a full-span plain flap-type control and a semispan tab attached to the trailing edge of the flap. The chords of the flap and tab were 25.4 and 12.7 percent of the chord of the basic wing, respectively, measured parallel to the plane of symmetry. The flap and tab gaps were approximately 0.3 and 0.1 percent of the wing chord, respectively.

The model was mounted on an electrical strain-gage balance enclosed within the transonic bump. The wing was attached to the balance mount through a wing-profile cutout in the turntable that forms part of the surface of the bump. Air flow between the wing root and the cutout was restricted by a sponge-rubber seal attached to the wing butt within the balance chamber. The shaft of the flap, collinear with the hinge line, extended through the turntable into the balance chamber and on this shaft within the chamber were two of the four hinges that supported the flap

and also the strain gage that measured the hinge moments of the flap-tab combination. In a similar manner, the tab strain gage and one of the three hinges supporting the tab were on the extended tab shaft within the bump chamber. The tab strain gage measured only the hinge moments of the tab, but the flap strain gage measured the hinge moments of the total area (flap plus tab) behind the flap hinge line. Flap and tab hinge moments and lift were measured simultaneously with calibrated potentiometers.

TESTS AND CORRECTIONS

The model was tested in the flow field of a transonic bump mounted on the floor of the Langley high-speed 7- by 10-foot tunnel. Typical contours of Mach number over the bump in the vicinity of model location with model removed are shown in figure 2. The test Mach number range was from 0.72 to 1.20 and the angle-of-attack range from -2° to 16°. Flap hinge moments were obtained through a deflection range of $\pm 20^\circ$ and tab hinge moments through a deflection range generally from a 10° unbalancing deflection to a 30° balancing deflection.

The variation with Mach number of mean test Reynolds number based on the mean aerodynamic chord is given in figure 3.

Wind-tunnel blockage and jet-boundary corrections were considered negligible because of the relative small size of the model compared to the size of the tunnel test section. Corrections to flap and tab deflections made necessary by shaft twist and strain-gage beam bending under loads have been applied to the data.

RESULTS AND DISCUSSION

Presentation of Data

The figures presenting the results of the investigation are as follows:

Figure	Variables	δ_f, deg	δ_t, deg
4	C_{h_f} against α	0	0
4	C_{h_t} against α	0	0
5	C_{h_t} against δ_f	–	0
6	C_{h_f} against δ_f	–	Various values

Figure	Variables	δ_f, deg	δ_t, deg
7	C_{h_t} against δ_t	Various values	-------
8	C_{h_f} against δ_t	0	-------
9	$C_{h_{t_{\delta_t}}}$ and $C_{h_{t_{\delta_f}}}$ against M	-------	-------
10	$C_{h_{f_{\delta_f}}}$ and $C_{h_{f_{\delta_t}}}$ against M	-------	-------
11	C_L, C_{h_t}, and δ_t against δ_f	$\Delta C_{h_f} = 0$	
12	C_L against α	0	0
13	C_L against δ_f	-------	0
13	C_L against δ_t	0	-------
14	$C_{L_{\delta_f}}$, $C_{L_{\delta_t}}$, and $\left(C_{L_{\delta_f}}\right)_{\Delta C_{h_{f=0}}}$ against M	-------	-------

Hinge-Moment Characteristics

As indicated in figure 4 and as expected, increasing angle of attack produced increasing negative hinge-moment coefficients of the undeflected flap and tab. An increase in Mach number also produced an increase in the magnitude of the hinge-moment coefficients at subsonic speeds but had little effect at supersonic speeds. The variation of tab and flap hinge-moment coefficients with flap deflections (figs. 5 and 6(a)) is nonlinear at subsonic speeds at or near zero angle of attack, but the variation tends to become more linear with increase in angle of attack or with increase in Mach number up to the maximum deflection tested. From figure 6 one may estimate the amount of flap deflection that a given tab deflection is able to balance for various angles of attack under steady flight conditions. The variation of tab hinge-moment coefficient with tab deflection is nearly linear between tab deflections of $\pm 10^\circ$ (fig. 7), and the flap hinge-moment coefficients produced by tab deflection (fig. 8) on the undeflected flap varies linearly with tab deflections between $\pm 10^\circ$.

From the data of figures 5 to 8, the hinge-moment parameters of the flap and tab were determined and they are presented in figures 9 and 10. The slopes were measured near zero deflection, and since many of the curves are nonlinear, design information for larger deflections should be obtained from the hinge-moment coefficient curves themselves rather than from the parameters. At small angles of attack of the wing, the parameters $C_{h_{t_{\delta_t}}}$, $C_{h_{t_{\delta_f}}}$, and $C_{h_{f_{\delta_f}}}$ approximately double in value as the Mach number increases from subsonic to supersonic, with the greatest

rate of increase occurring near $M = 1$. The parameter $C_{h_{f_{\delta_t}}}$, which indicates the balancing power of the tab, also shows increased values supersonically over subsonic conditions, but the percentage increase is generally much less than for the aforementioned parameters. The ratio of $C_{h_{f_{\delta_f}}}$ to $C_{h_{f_{\delta_t}}}$ is an indication of the ratio of tab deflection to flap deflection (δ_t/δ_f) necessary for balancing the flap hinge moments produced by flap deflection. Figure 10 indicates that a tab-flap deflection ratio of approximately 1 will enable the tab to balance flap hinge moments produced by flap deflection at subsonic speeds, but at supersonic speeds a ratio of approximately 1.5 will be necessary except at high angles of attack. These ratios should hold for small deflections, but since the slopes of the flap hinge-moment curves resulting from tab deflection (fig. 8) decrease at large deflections while the slopes of the flap hinge-moment curves resulting from flap deflection (fig. 6(a)) either remain constant or increase at large deflections, one may expect that a larger tab-flap deflection ratio will be required for balance at the larger flap deflections.

In order to give some indication of results at larger deflections at zero angle of attack, figure 11 was prepared after taking into account corrections to tab and flap deflections through a series of cross plots. The curves of δ_t against δ_f are practically linear for flap deflections between $\pm 10^\circ$, but the slopes increase very sharply for larger deflections. The curves of C_{h_t} against δ_f (fig. 11) may be used to determine the hinge-moment force to be overcome by some device attached to the flap and actuating the tab, since the tab hinge-moment coefficients are the coefficients of the tab when the tab is deflected sufficiently to nullify flap hinge moments produced by any indicated flap deflection. For example, the results of applying the data of this investigation to a full-scale fighter plane with a horizontal tail, similar to the configuration tested, indicate that 10° deflection of the tabs on both elevators of 5.1 square-foot area each will result in a tab hinge moment of about 200 foot-pounds at sea level at $M = 1$, or slightly less than 100 foot-pounds at a 20,000-foot altitude.

The above discussion of tab-flap deflection ratios does not take into consideration the effect of changing angle of attack on the hinge moments. As indicated in figure 4, increasing angle of attack of the wing results in increasing negative hinge moments of the tab and flap, analogous to the effect of tab or flap deflection on hinge moments. In maneuvering flight, deflection of the control (aileron or elevator) produces a translation of the control resulting in a change in angle of attack of the control opposite to the change in angle of attack produced by the deflection. Hence, in maneuvering flight, the amount of control hinge moment at a given deflection to be balanced by the tab will be less than in steady flight.

Lift Characteristics

The lift characteristics of the wing with flap and tab undeflected are presented in figure 12. The lift coefficients of figure 12 are faired values obtained from figure 13.

Since the balancing force of the tab is obtained by deflecting it oppositely to the flap, the lift effectiveness of the flap is reduced by tab deflection. The net lift parameter of the flap with a tab-flap deflection ratio sufficient to balance the flap hinge moment produced by flap deflection is obtained from the following relation of the parameters obtained by measuring slopes near zero deflection:

$$\left(C_{L_{\delta_f}}\right)_{\Delta C_{h_{f=0}}} = C_{L_{\delta_f}} - \frac{\delta_t}{\delta_f} C_{L_{\delta_t}}$$

where

$$\frac{\delta_t}{\delta_f} = \frac{C_{h_{f_{\delta_f}}}}{C_{h_{f_{\delta_t}}}}$$

The lift parameters $C_{L_{\delta_f}}$ and $C_{L_{\delta_t}}$ obtained from figure 13 and the net lift parameter obtained from the relation above are given in figure 14. In general, the lift parameters decrease some with Mach number except at high angles of attack and decrease with increasing angle of attack, except the tab lift parameter, which shows some increases. The net lift parameter of the balanced control $\left(C_{L_{\delta_f}}\right)_{\Delta C_{h_{f=0}}}$ is about 80 percent of the lift parameter of the unbalanced control $C_{L_{\delta_f}}$ at zero angle of attack but drops to about 67 percent at $\alpha = 16^\circ$. The net lift coefficient of the balanced flap for larger deflections at zero angle of attack is indicated in figure 11. The lift coefficient varies linearly with deflection for flap deflections between roughly $\pm 10^\circ$. It should be stated, though, that the values given in figure 11 were based on the indicated δ_f for which C_{h_f} was zero, and since δ_f was obtained from curves (fig. 6) that had been determined by as few as two test points, the values at large deflections in figure 11 probably are not sufficiently reliable for design purposes but are presented only to give an indication of the effectiveness of the tab.

CONCLUSIONS

A wind-tunnel investigation at transonic speeds was made to determine the lift and hinge-moment characteristics of a 7.6-percent-thick, 45.6° sweptback wing of aspect ratio 3, having a full-span flap and an inboard tab with chord and span one-half the chord and span of the flap, and attached to the trailing edge of the flap. Conclusions based on the investigation are as follows:

1. In order for the tab to balance the flap, a tab-flap deflection ratio of approximately 1 at subsonic speeds and a ratio of 1.5 at supersonic speeds was indicated, based on small deflections and steady flight.

2. The lift effectiveness of the balanced flap was about 80 percent of the value of the unbalanced flap at zero angle of attack but decreased to about 67 percent at 16° angle of attack.

3. At supersonic speeds, the rates of change of flap hinge moment with flap deflection, tab hinge moment with tab deflection, and tab hinge moment with flap deflection were approximately double the rates at subsonic speeds, but the rate of change of flap hinge moment with tab deflection varied less with Mach number than the aforementioned parameters.

Langley Aeronautical Laboratory,
National Advisory Committee for Aeronautics,
Langley Field, Va., October 14, 1954.

REFERENCES

1. Lockwood, Vernard E., and Hagerman, John R.: Aerodynamic Characteristics at Transonic Speeds of a Tapered 45° Sweptback Wing of Aspect Ratio 3 Having a Full-Span Flap Type of Control With Overhang Balance. Transonic-Bump Method. NACA RM L51L11, 1952.

2. Lowry, John G., and Fikes, Joseph E.: Preliminary Investigation of Control Characteristics at Transonic Speeds of a Tapered 45° Sweptback Wing of Aspect Ratio 3 Having a Horn-Balanced Full-Span Control. NACA RM L52A11, 1952.

3. Lockwood, Vernard E., and Fikes, Joseph E.: Preliminary Investigation at Transonic Speeds of the Effect of Balancing Tabs on the Hinge-Moment and Other Aerodynamic Characteristics of a Full-Span Flap on a Tapered 45° Sweptback Wing of Aspect Ratio 3. NACA RM L52A23, 1952.

4. Lockwood, Vernard E., and Fikes, Joseph E.: Investigation at Transonic Speeds of the Effect of a Positive-Lift Balancing Tab on the Hinge-Moment and Lift Characteristics of a Full-Span Flap on a Tapered 45° Sweptback Wing of Aspect Ratio 3. NACA RM L52J09, 1952.

5. Johnson, Harold I., and Brown, B. Porter: Measurements of Aerodynamic Characteristics of a 35° Sweptback NACA 65-009 Airfoil Model With $\frac{1}{4}$-Chord Bevelled-Trailing-Edge Flap and Trim Tab by the NACA Wing-Flow Method. NACA RM L9K11, 1950.

6. Lord, Douglas R., and Czarnecki, K. R.: Recent Information on Flap and Tip Controls. NACA RM L53I17a, 1953.

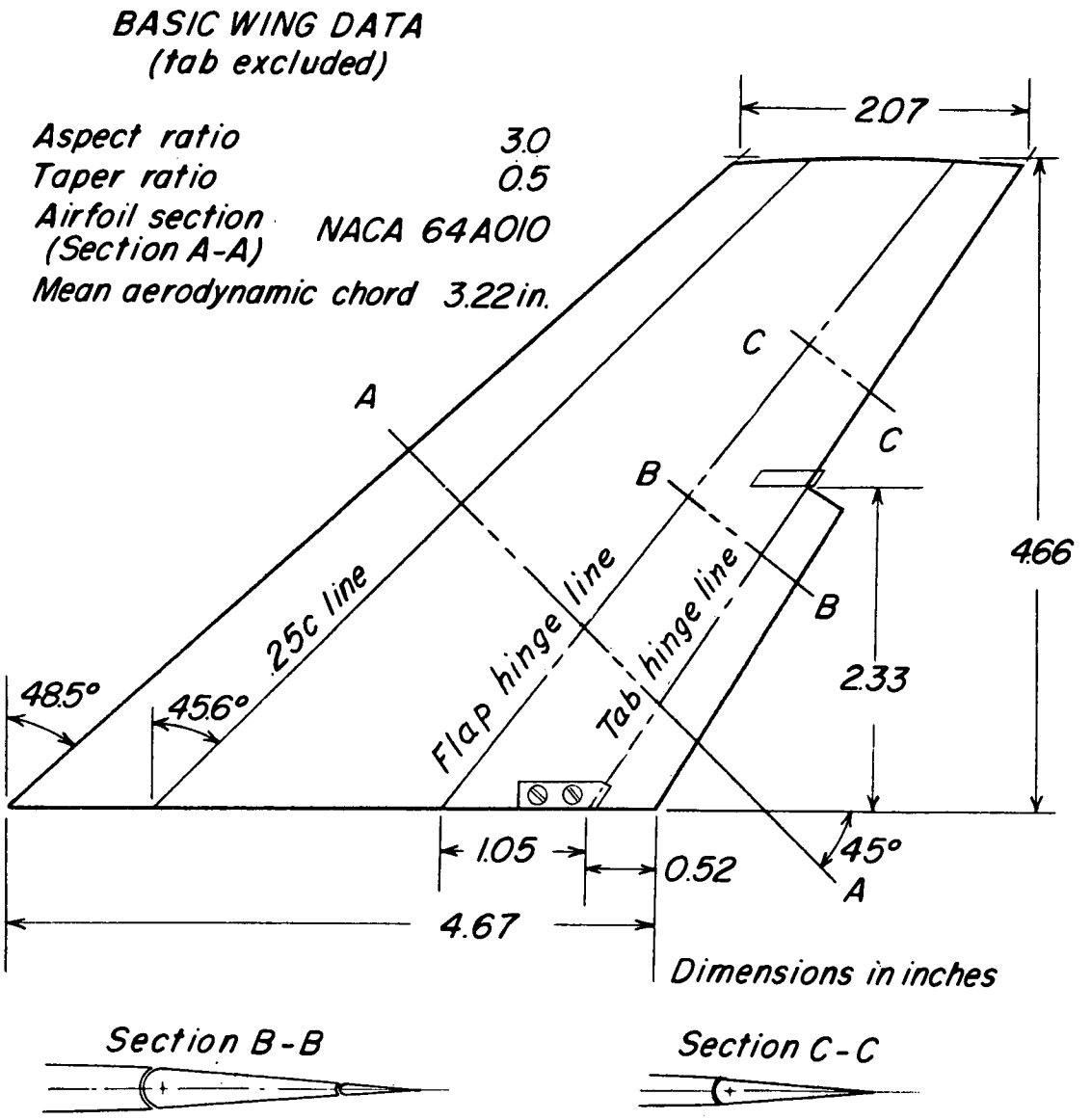

Figure 1.- Geometric characteristics of the model.

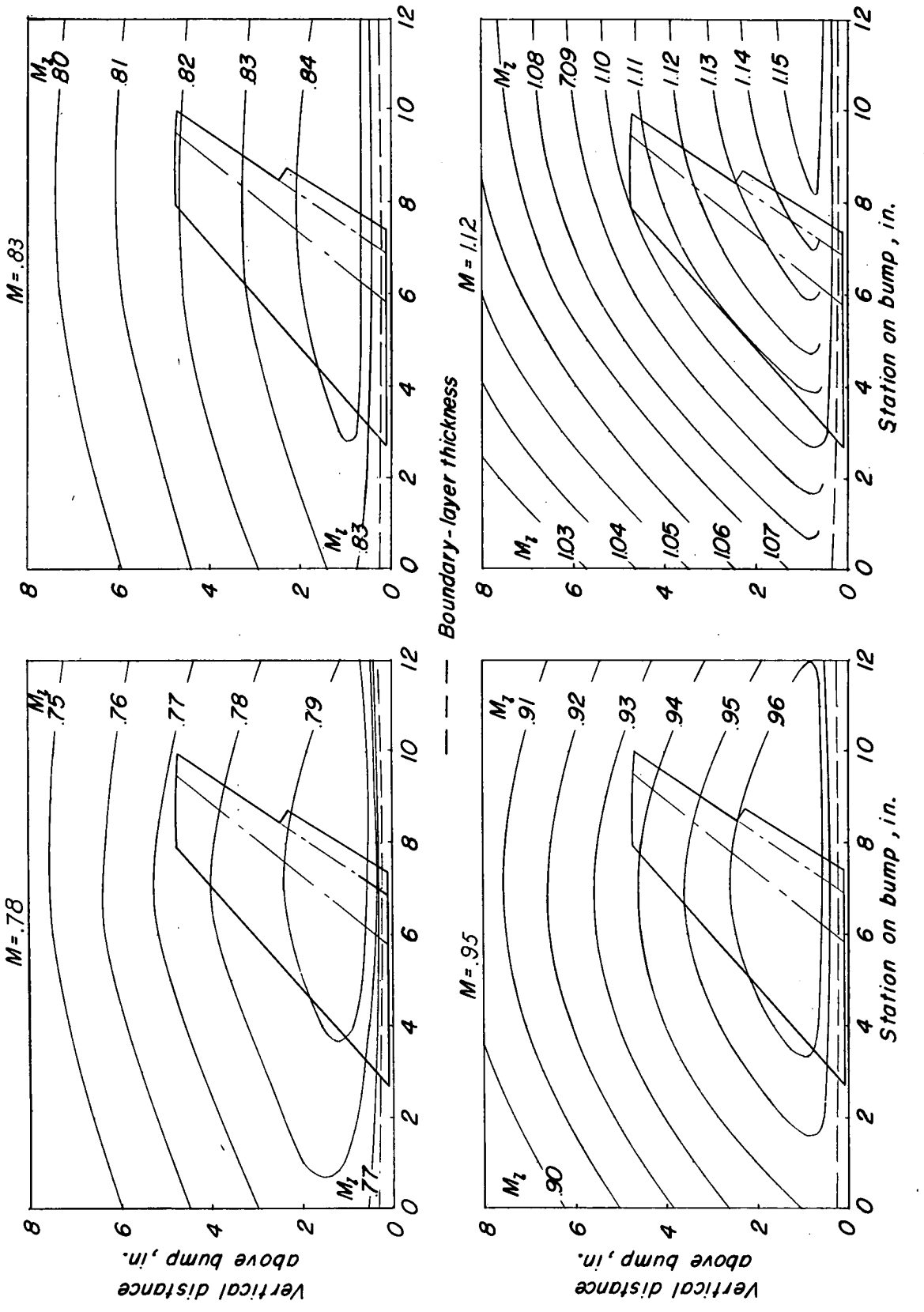

Figure 2.- Typical Mach number contours over transonic bump in region of model location.

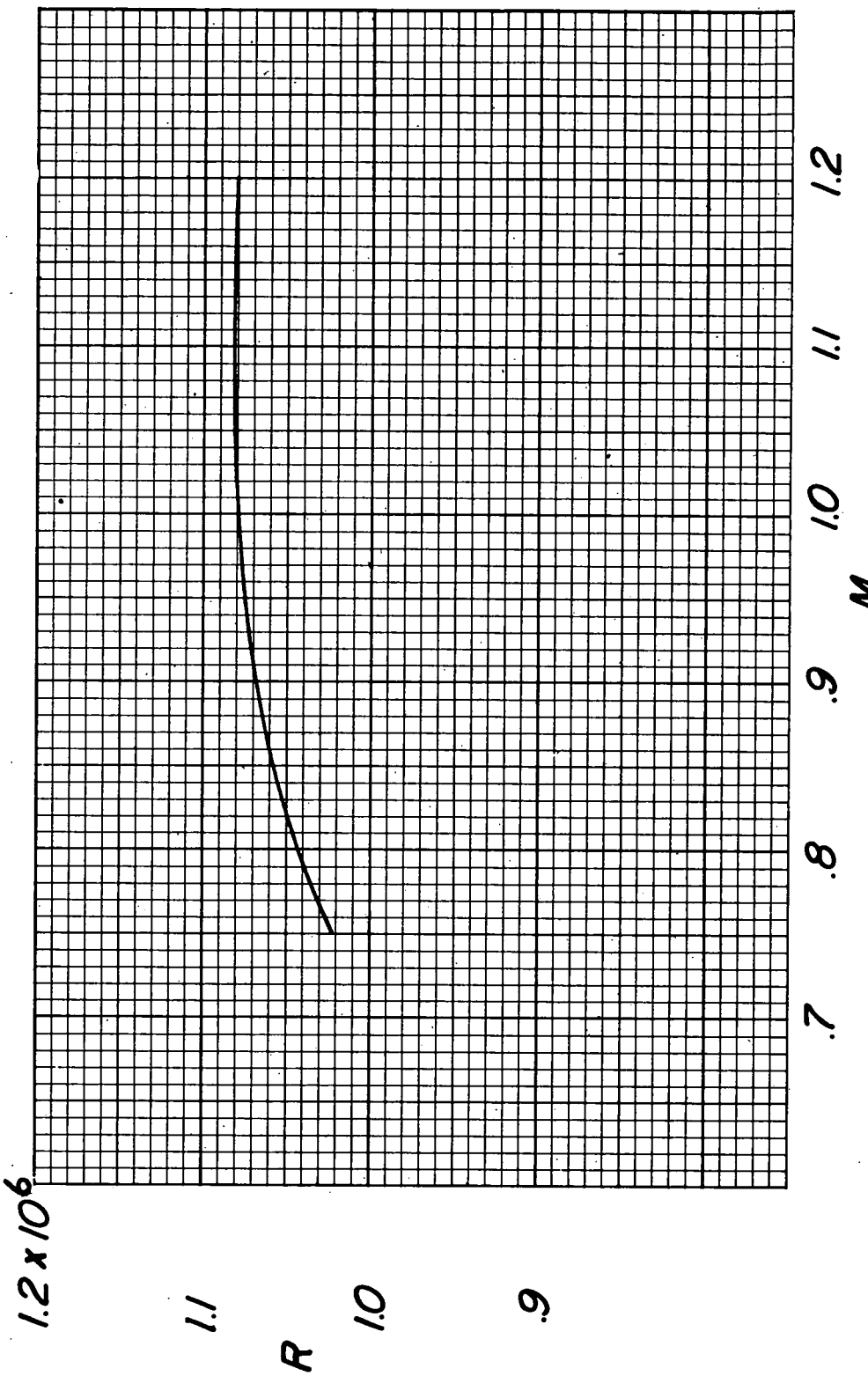

Figure 3.- Variation of mean Reynolds number with Mach number.

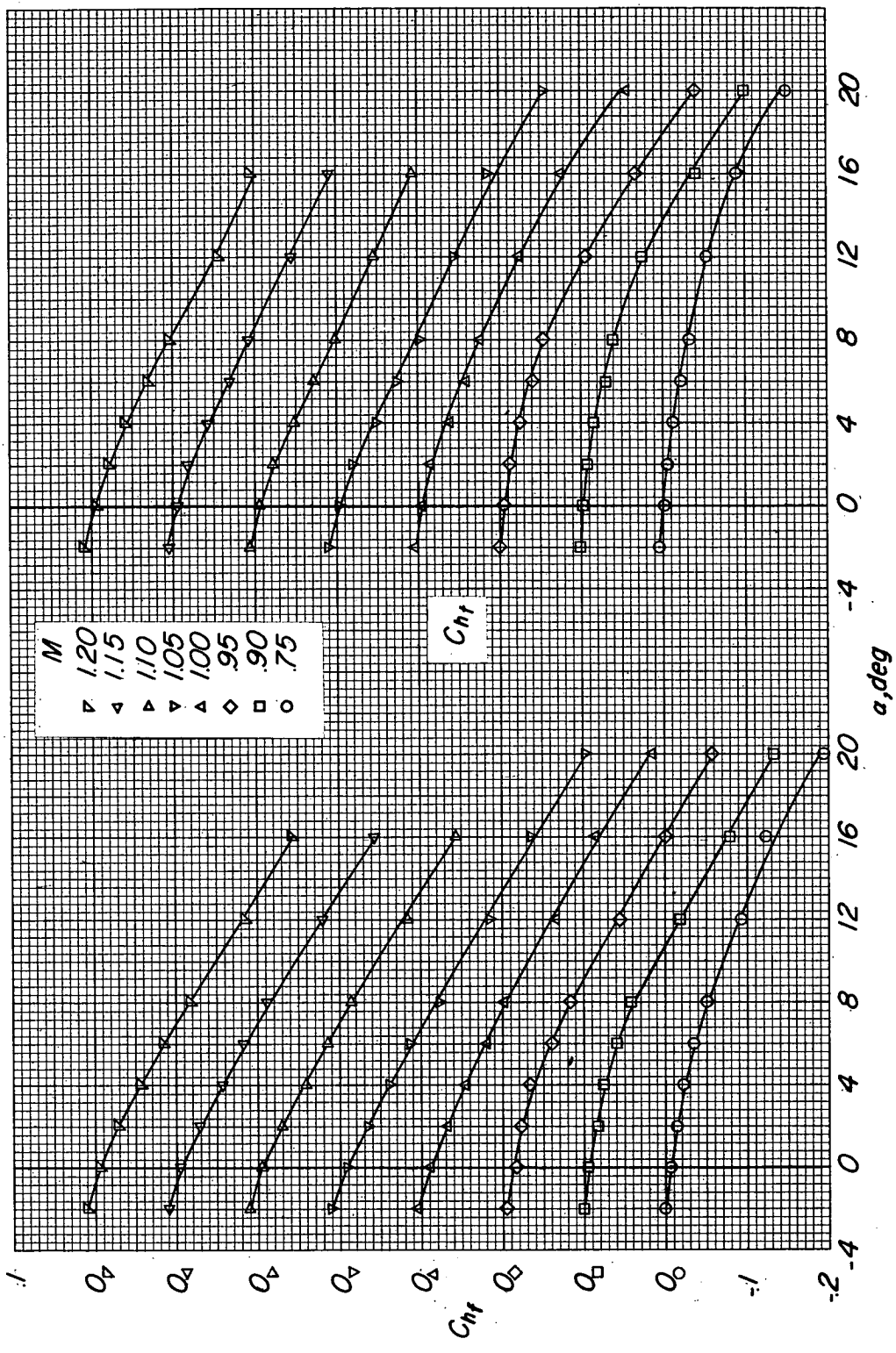

Figure 4.- Effect of angle of attack on flap hinge moments and on tab hinge moments. $\delta_f \approx 0°$; $\delta_t \approx 0°$.

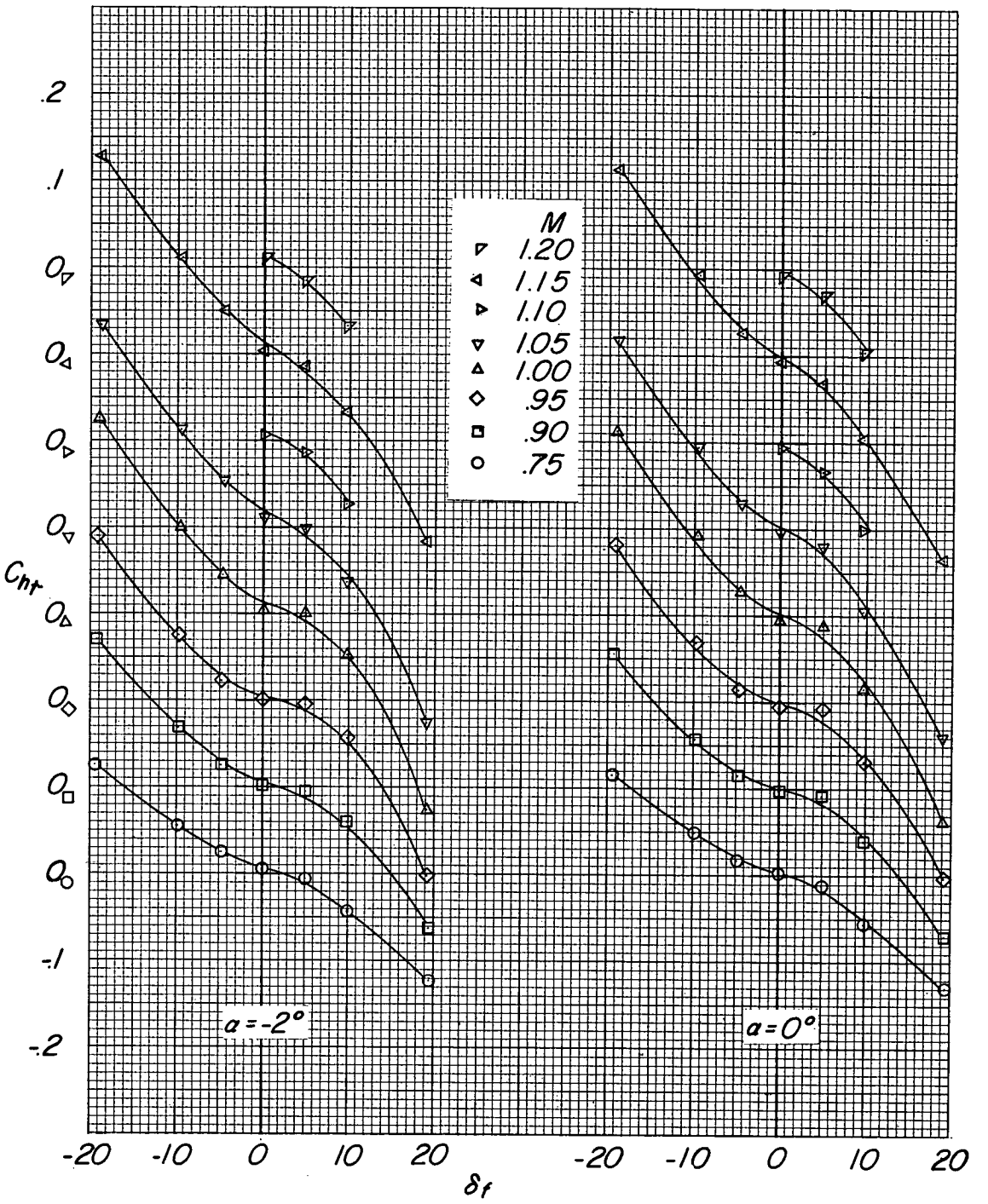

Figure 5.- Variation of tab hinge-moment coefficient with flap deflection for various Mach numbers and angles of attack. $\delta_t \approx 0^\circ$.

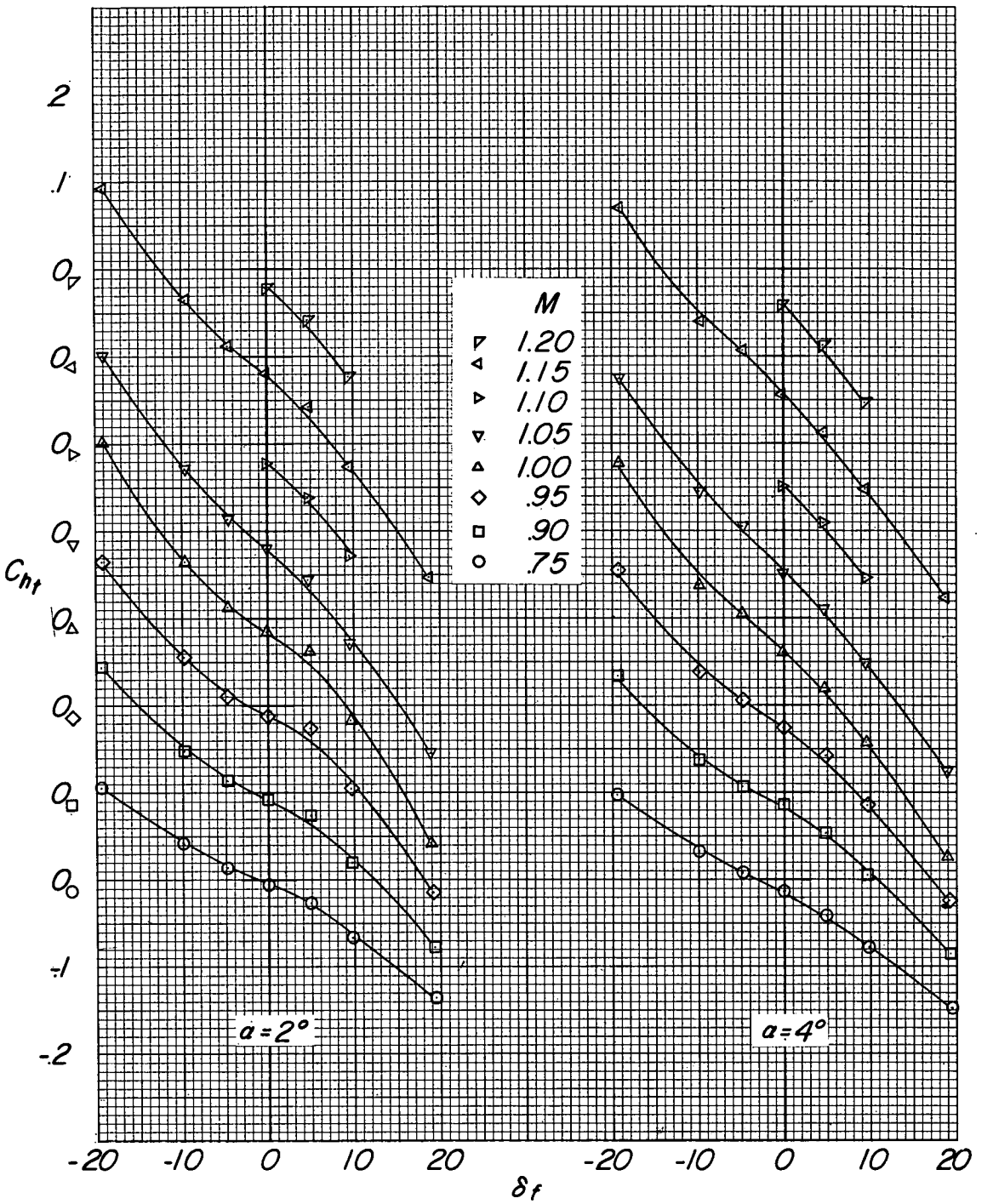

Figure 5.- Continued.

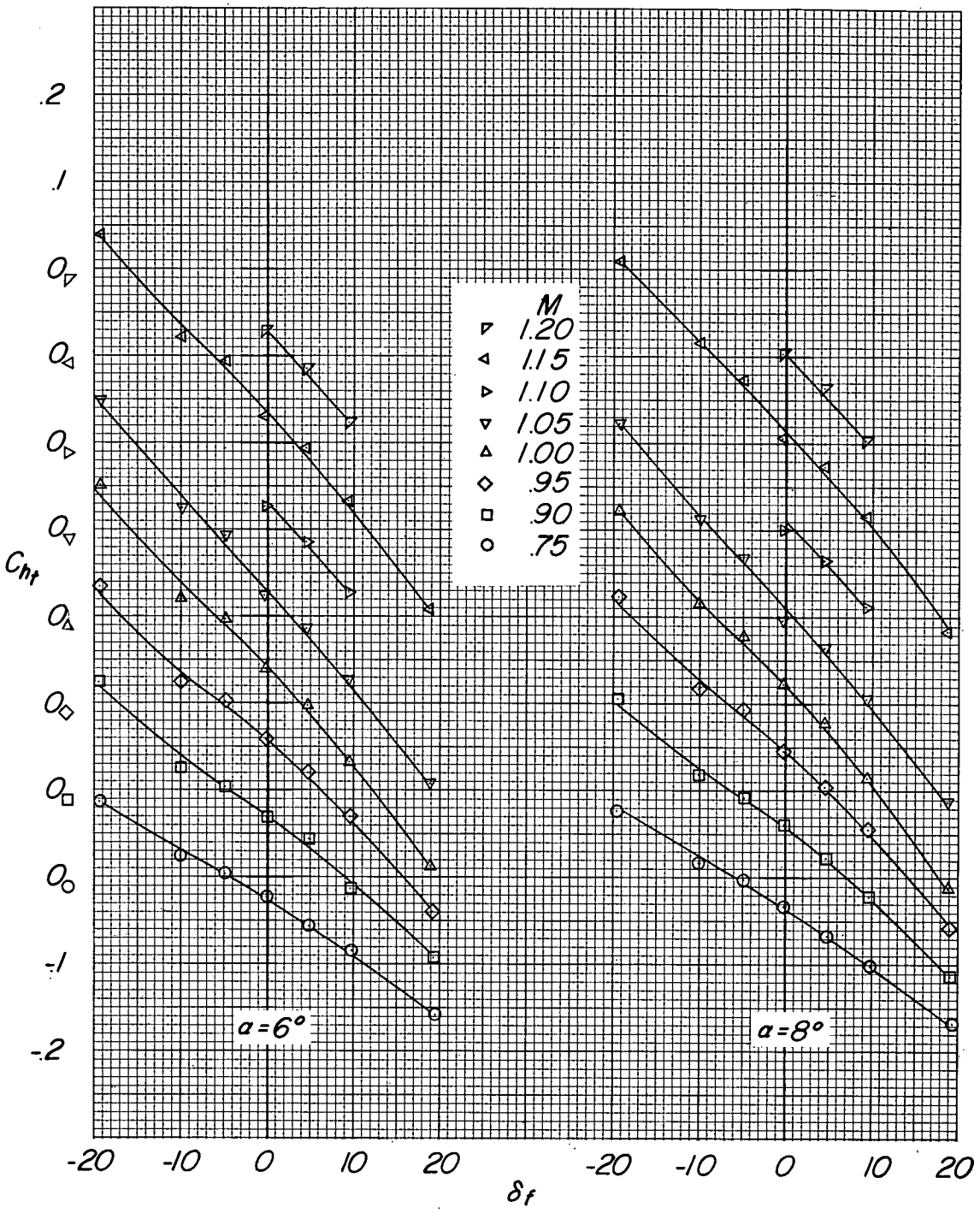

Figure 5.- Continued.

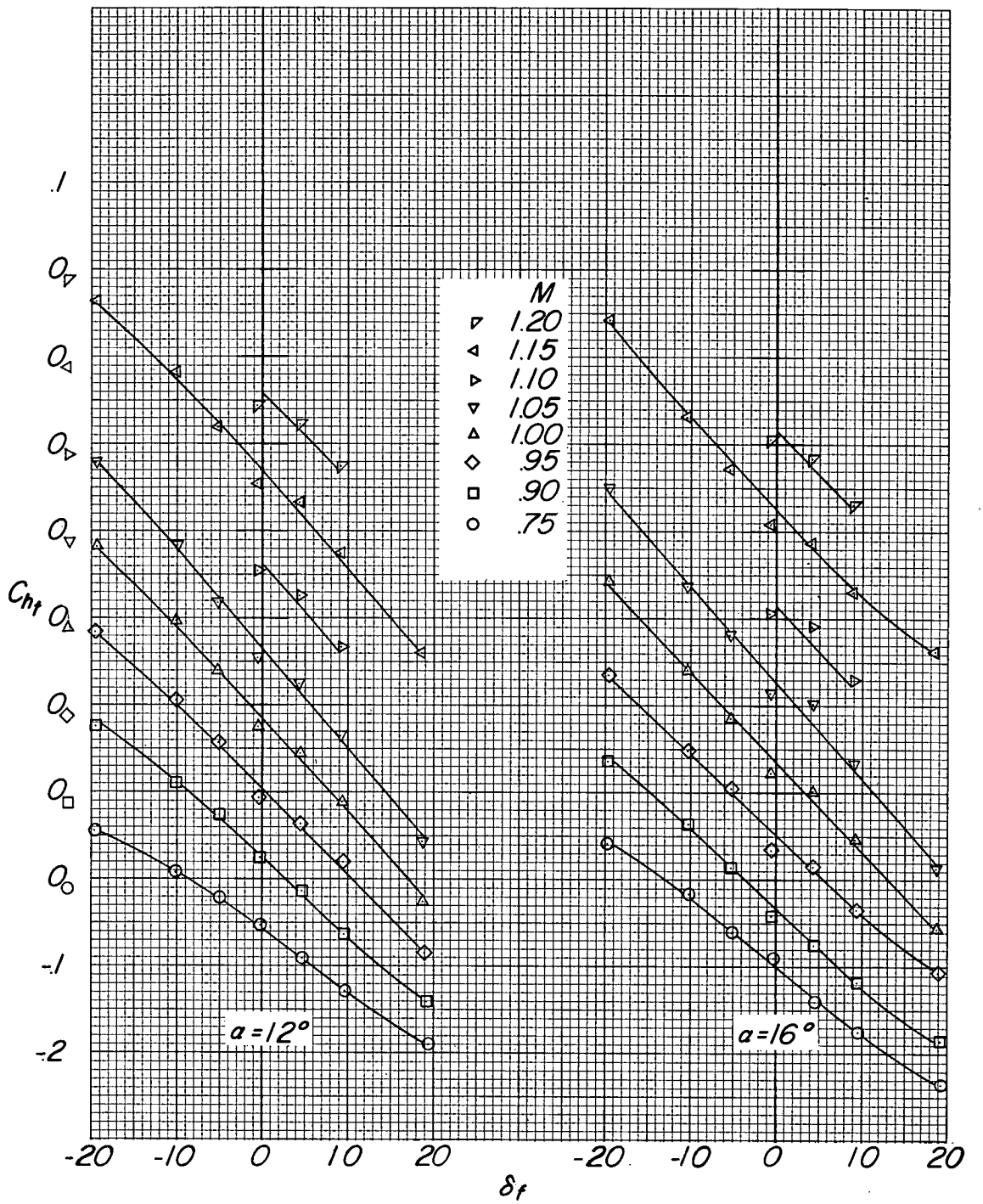

Figure 5.- Concluded.

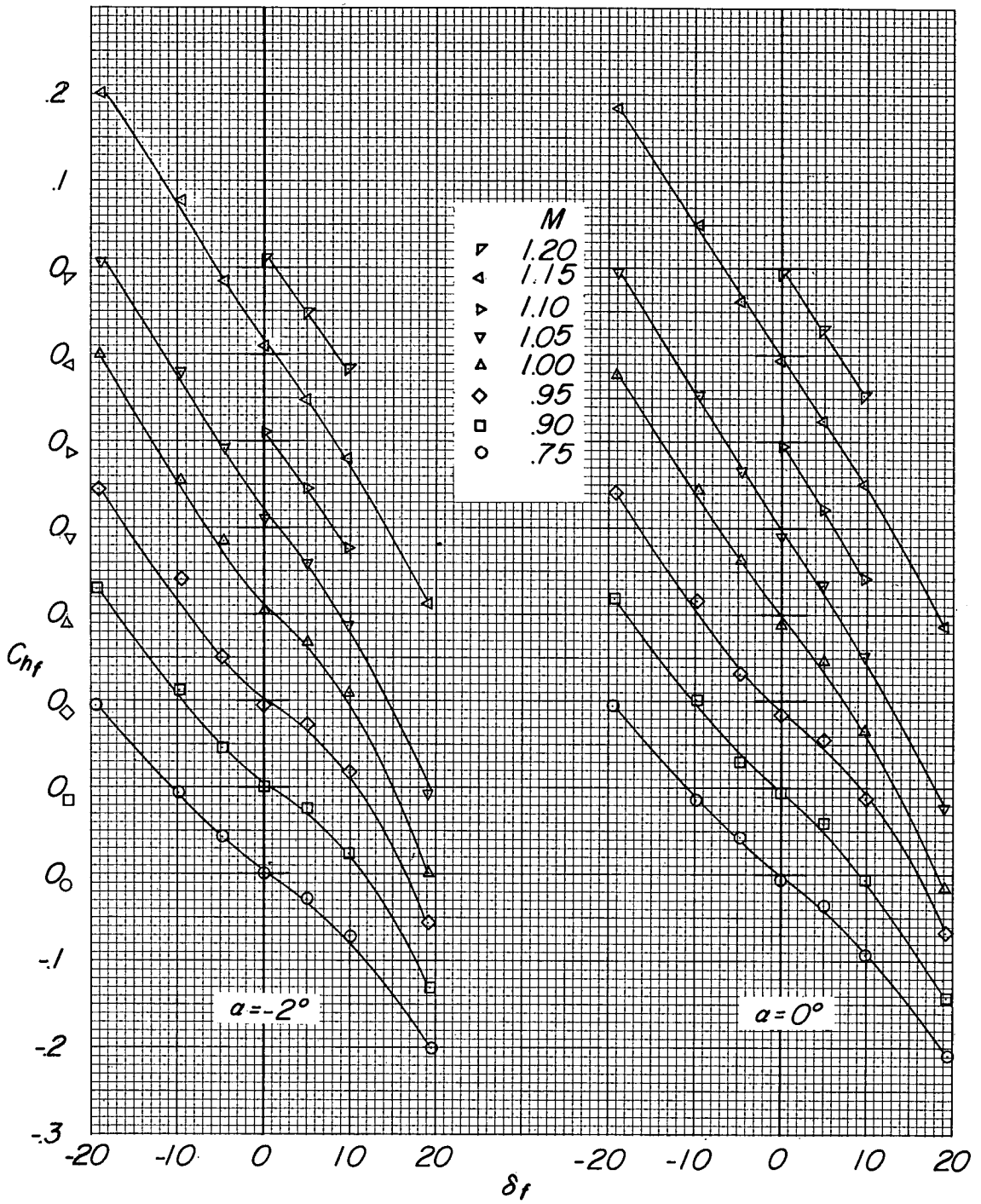

(a) $\delta_t \approx 0°$.

Figure 6.- Variation of flap hinge-moment coefficient with flap deflection for various Mach numbers, angles of attack, and tab deflections.

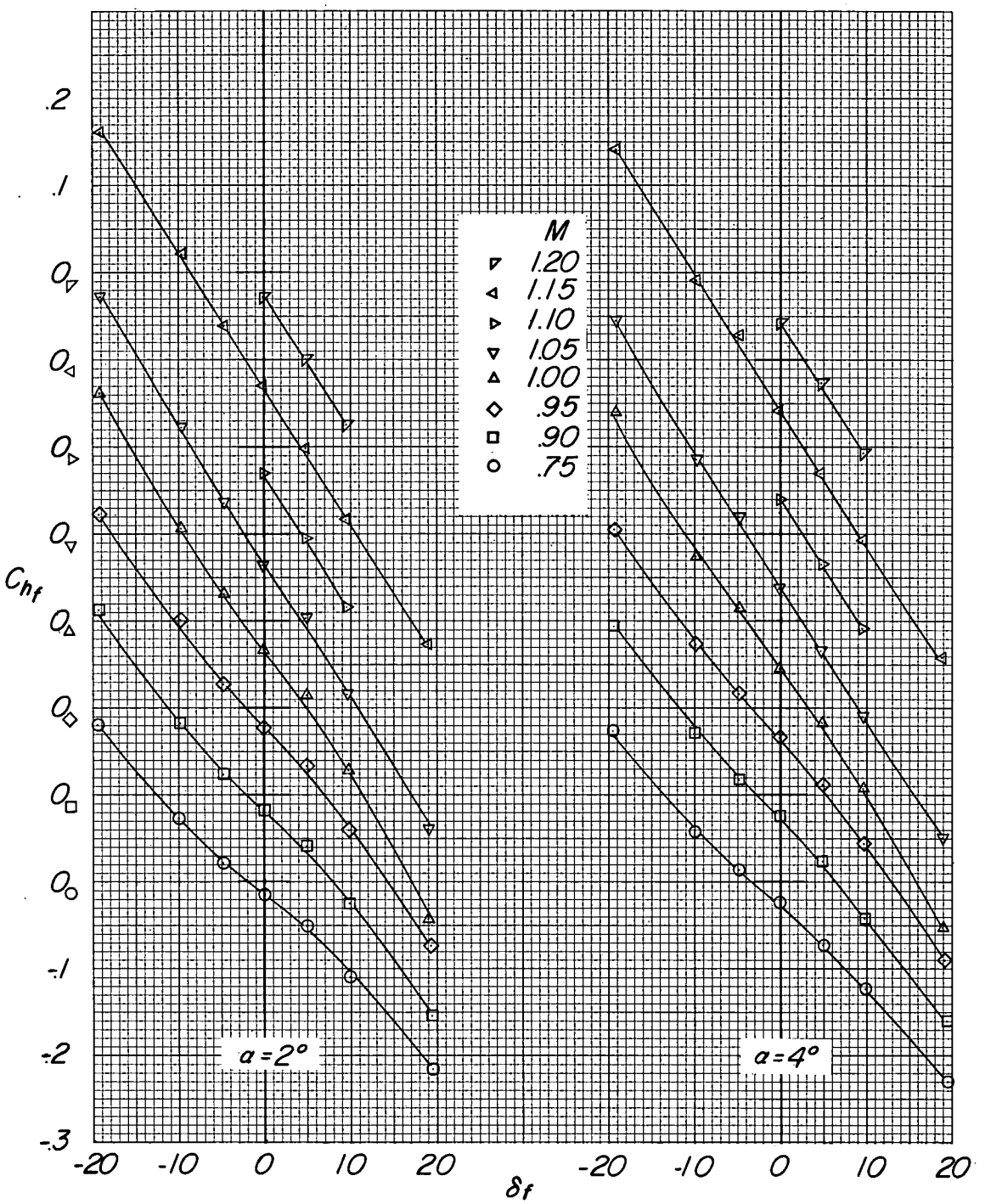

(a) Continued.

Figure 6.- Continued.

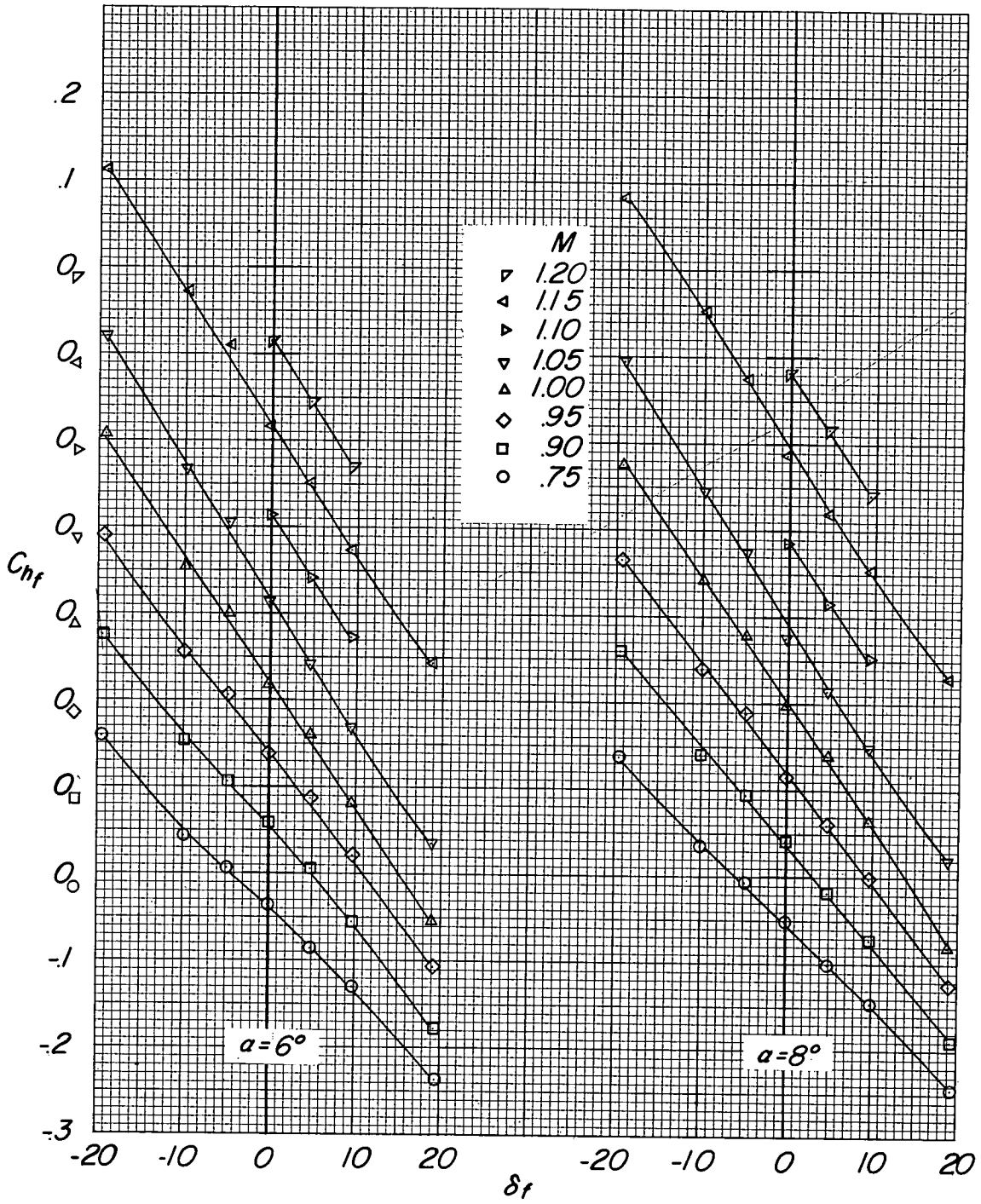

(a) Continued.

Figure 6.- Continued.

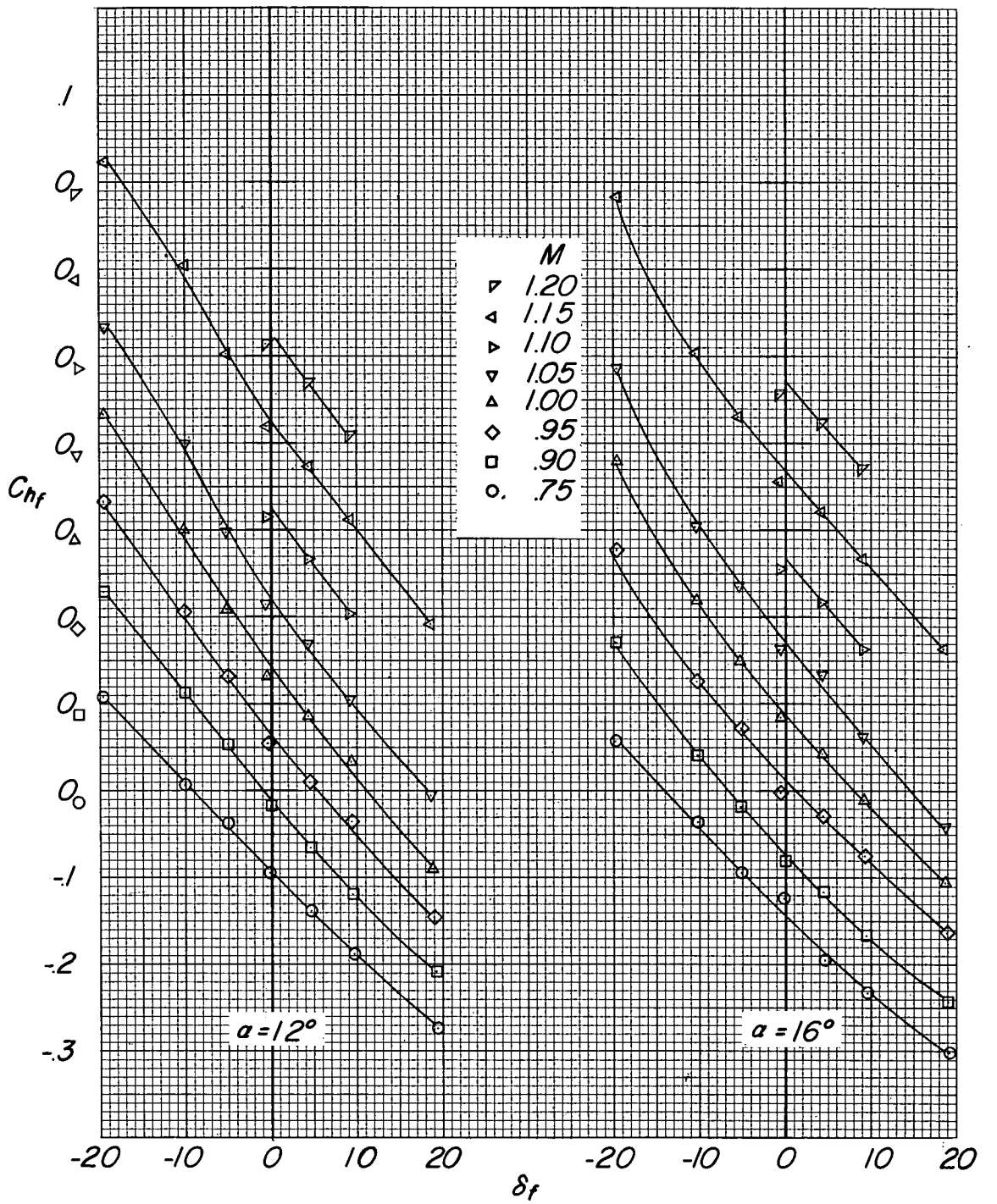

(a) Concluded.

Figure 6.- Continued.

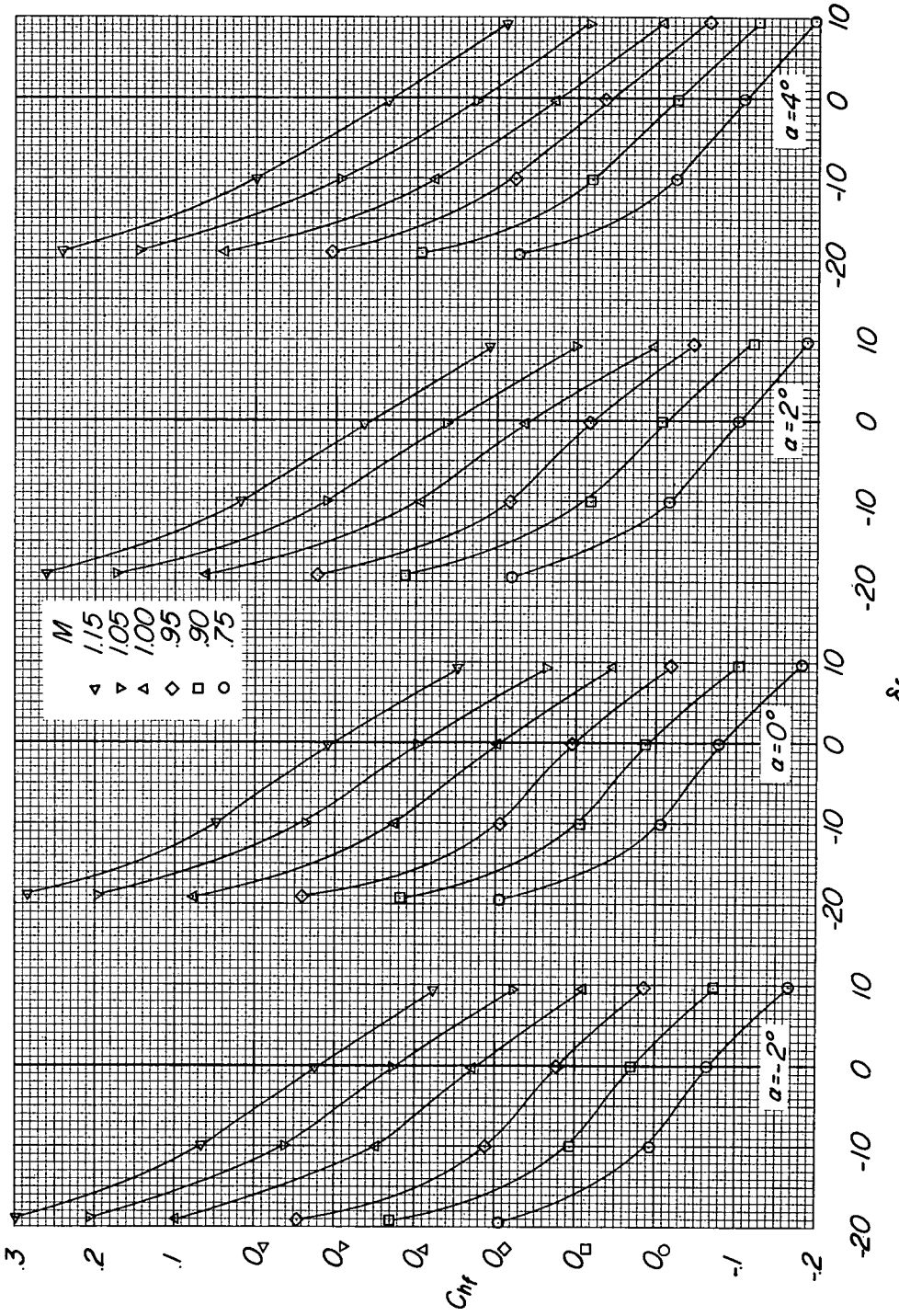

(b) $\delta_t \approx 9.4°$.

Figure 6.- Continued.

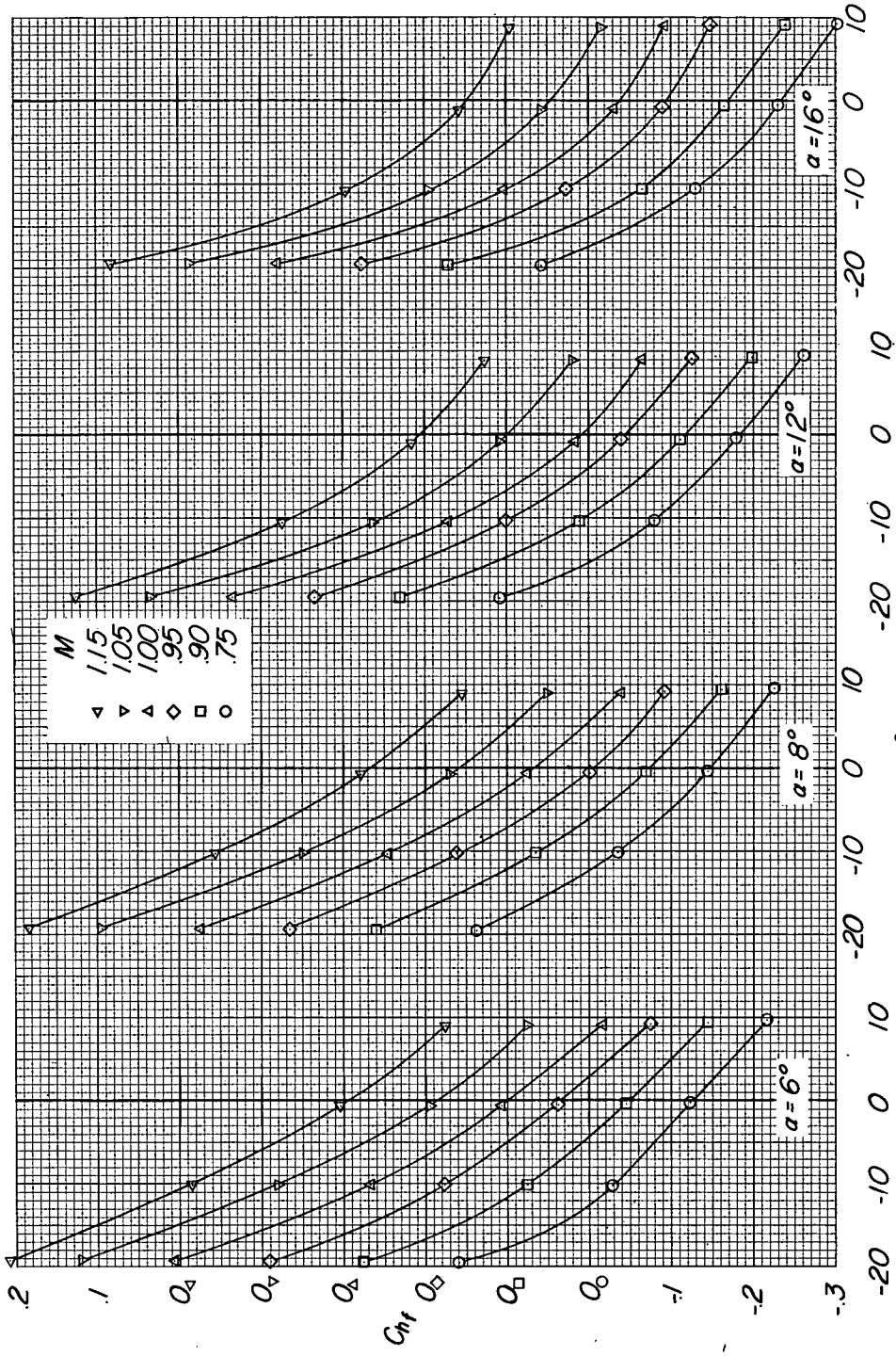

(b) Concluded.

Figure 6.- Continued.

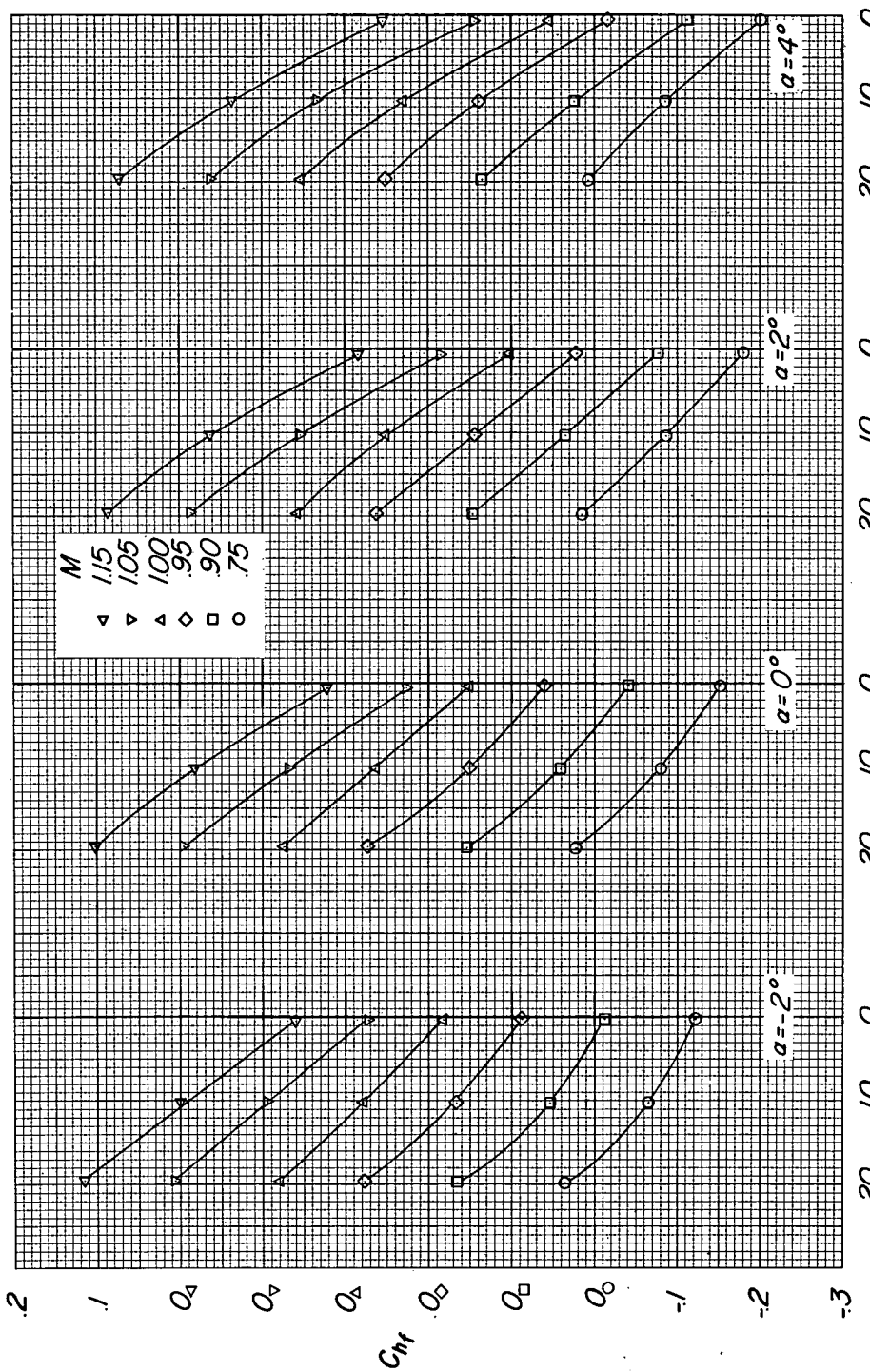

(c) $\delta_t \approx 19.4°$.

Figure 6.- Continued.

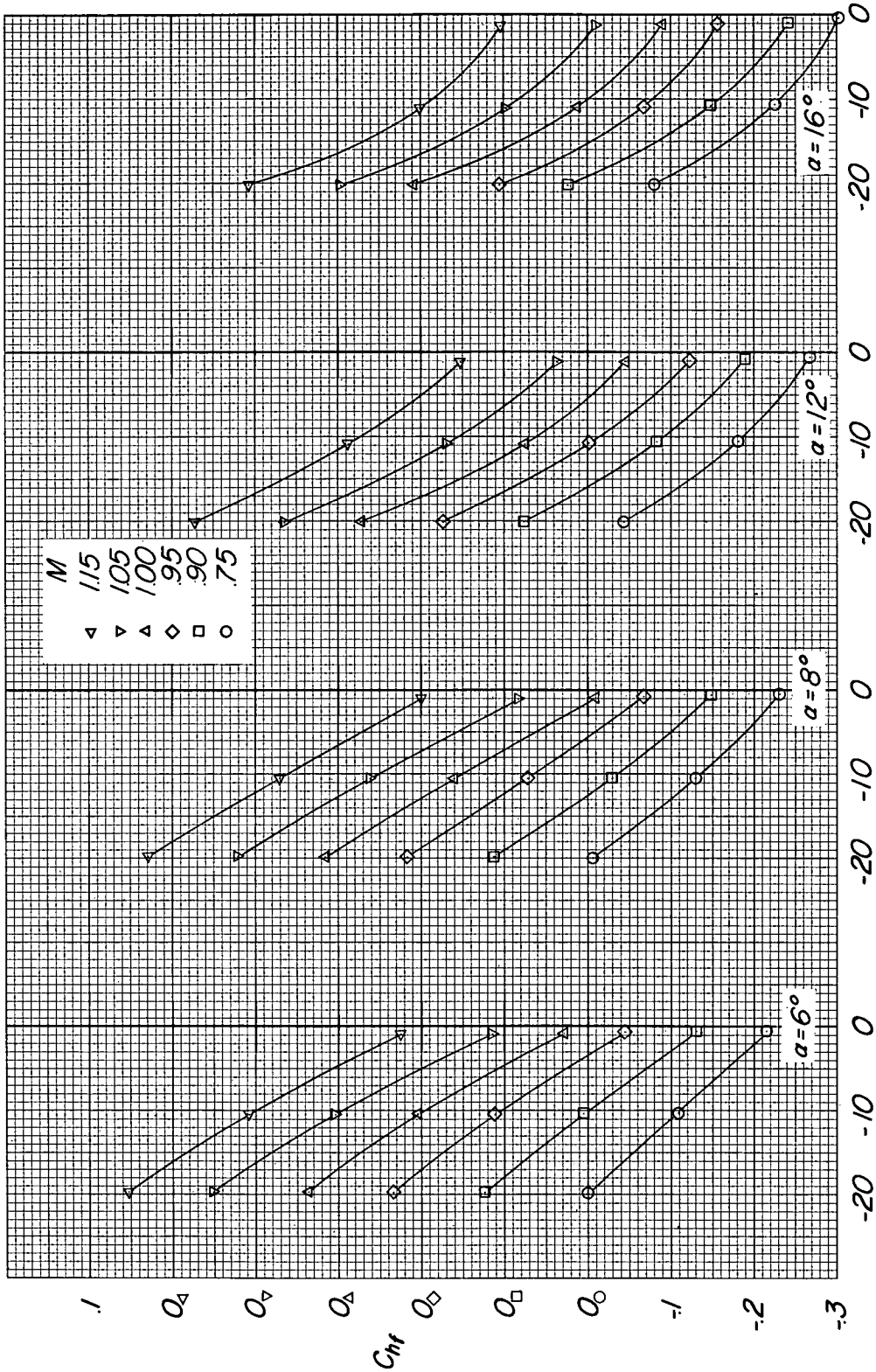

(c) Concluded.

Figure 6.- Continued.

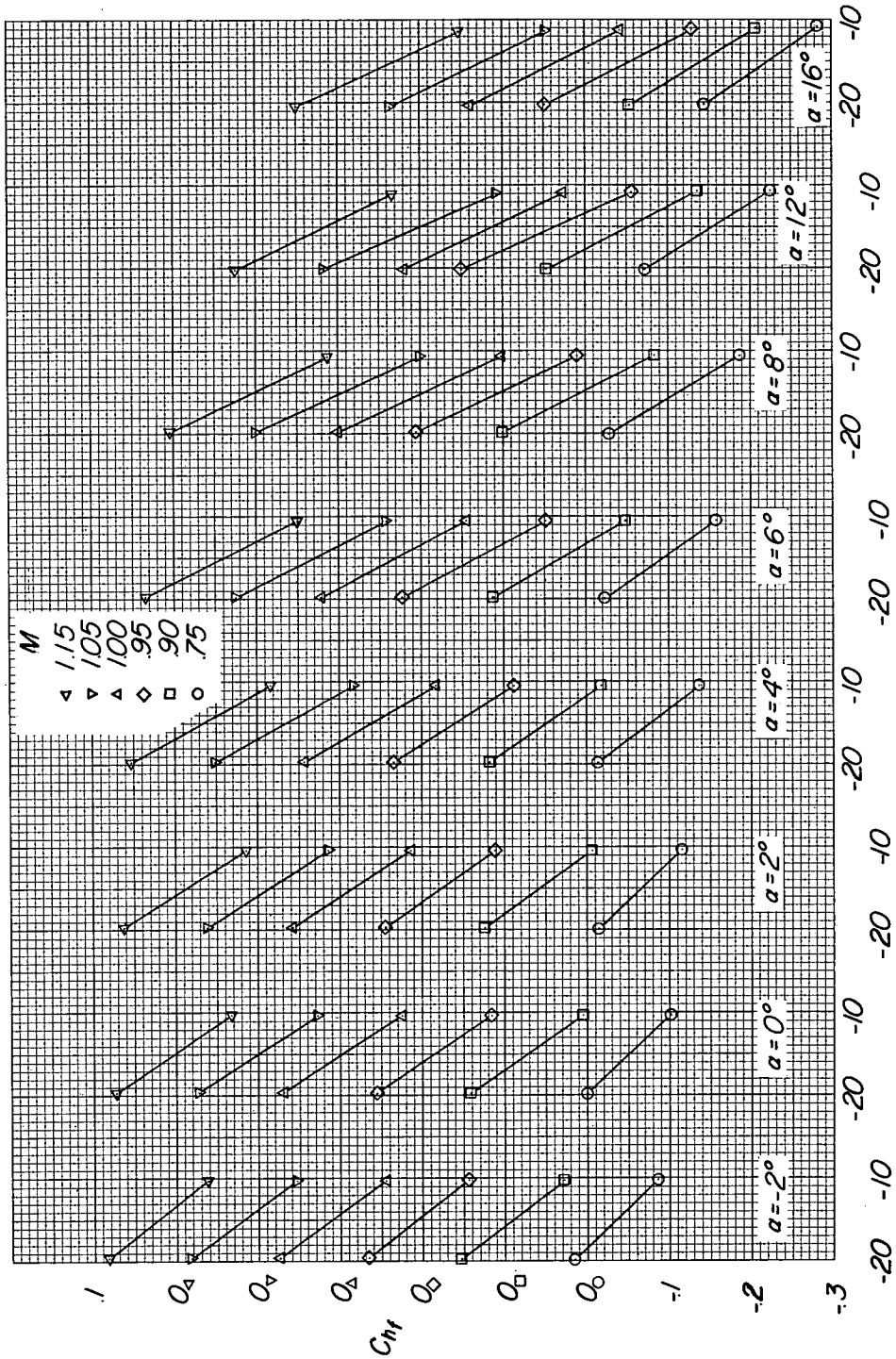

(d) $\delta_t \approx 29.9°$.

Figure 6.- Continued.

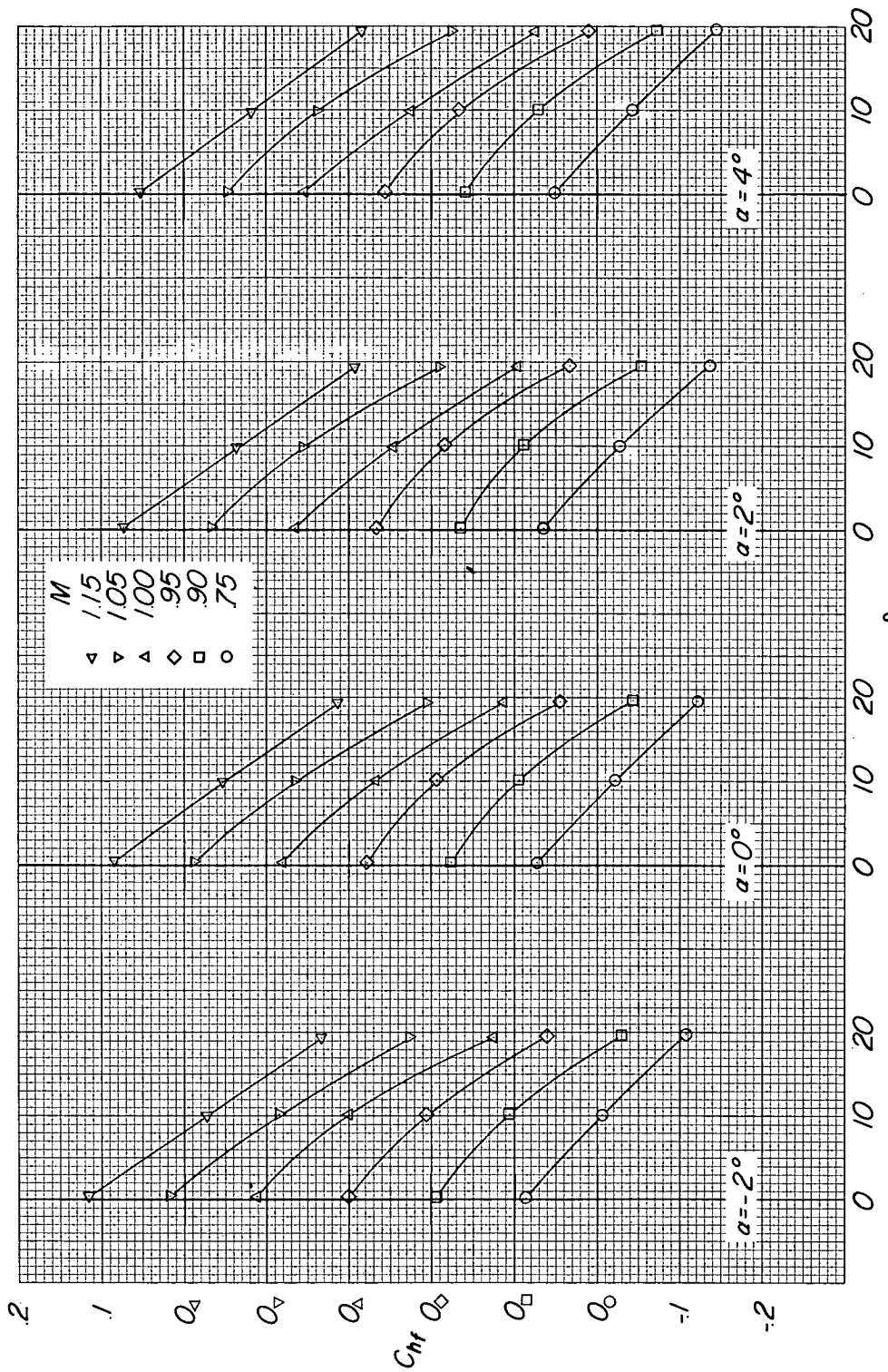

(e) $\delta_t \approx -10.2°$.

Figure 6.- Continued.

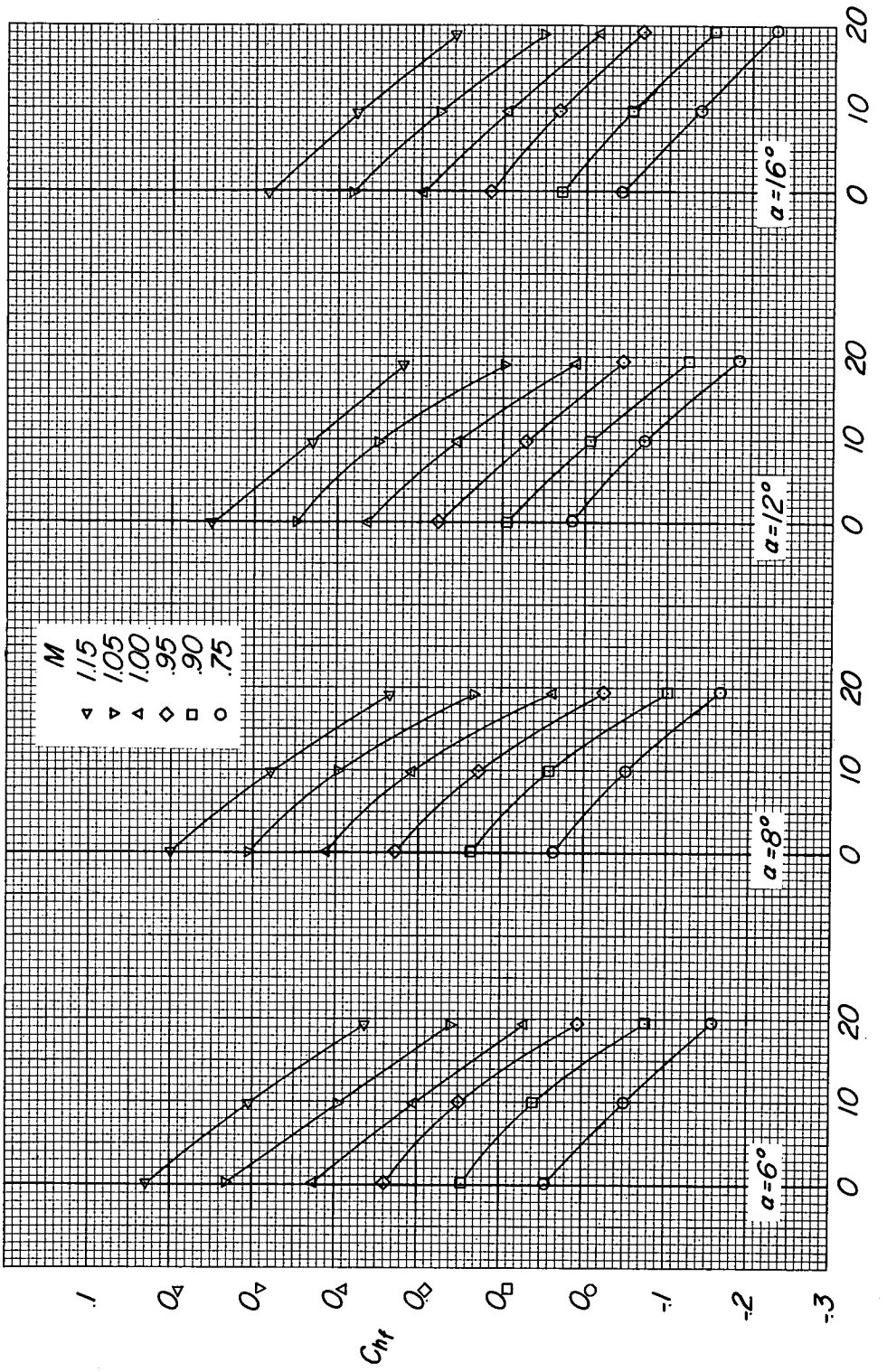

(e) Concluded.

Figure 6.- Continued.

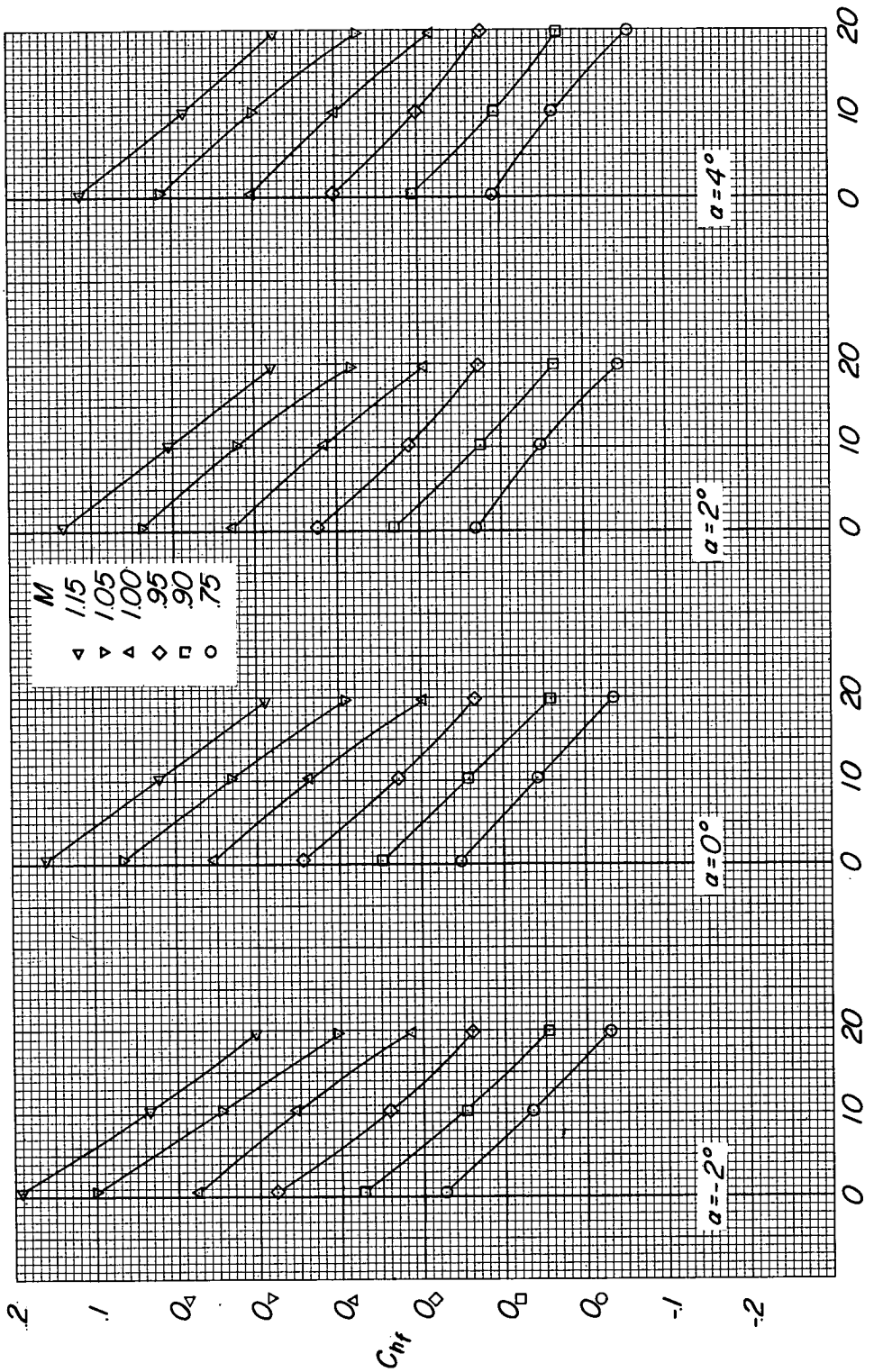

(f) $\delta_t \approx -19.5°$.

Figure 6.- Continued.

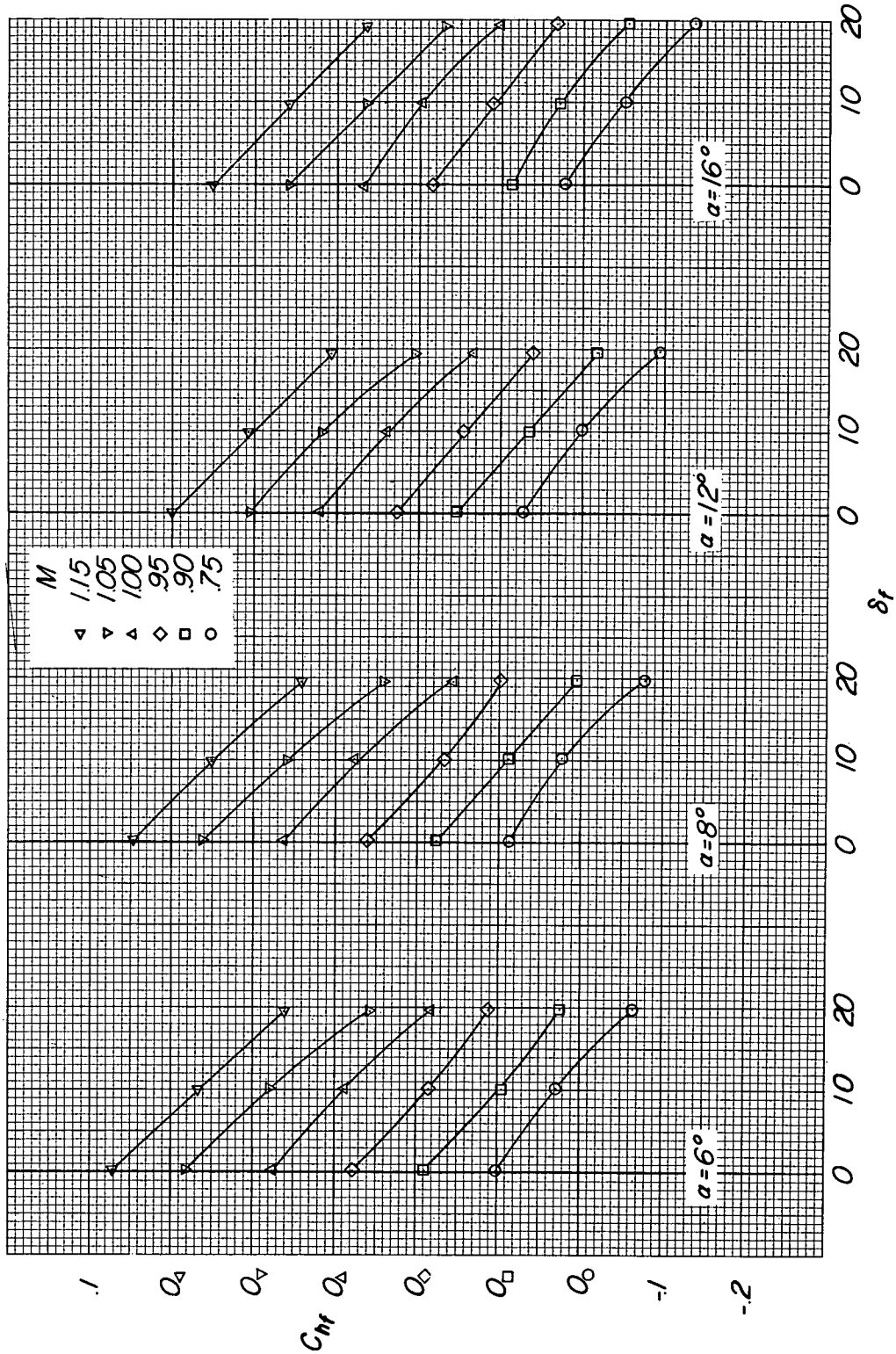

(f) Concluded.

Figure 6.- Continued.

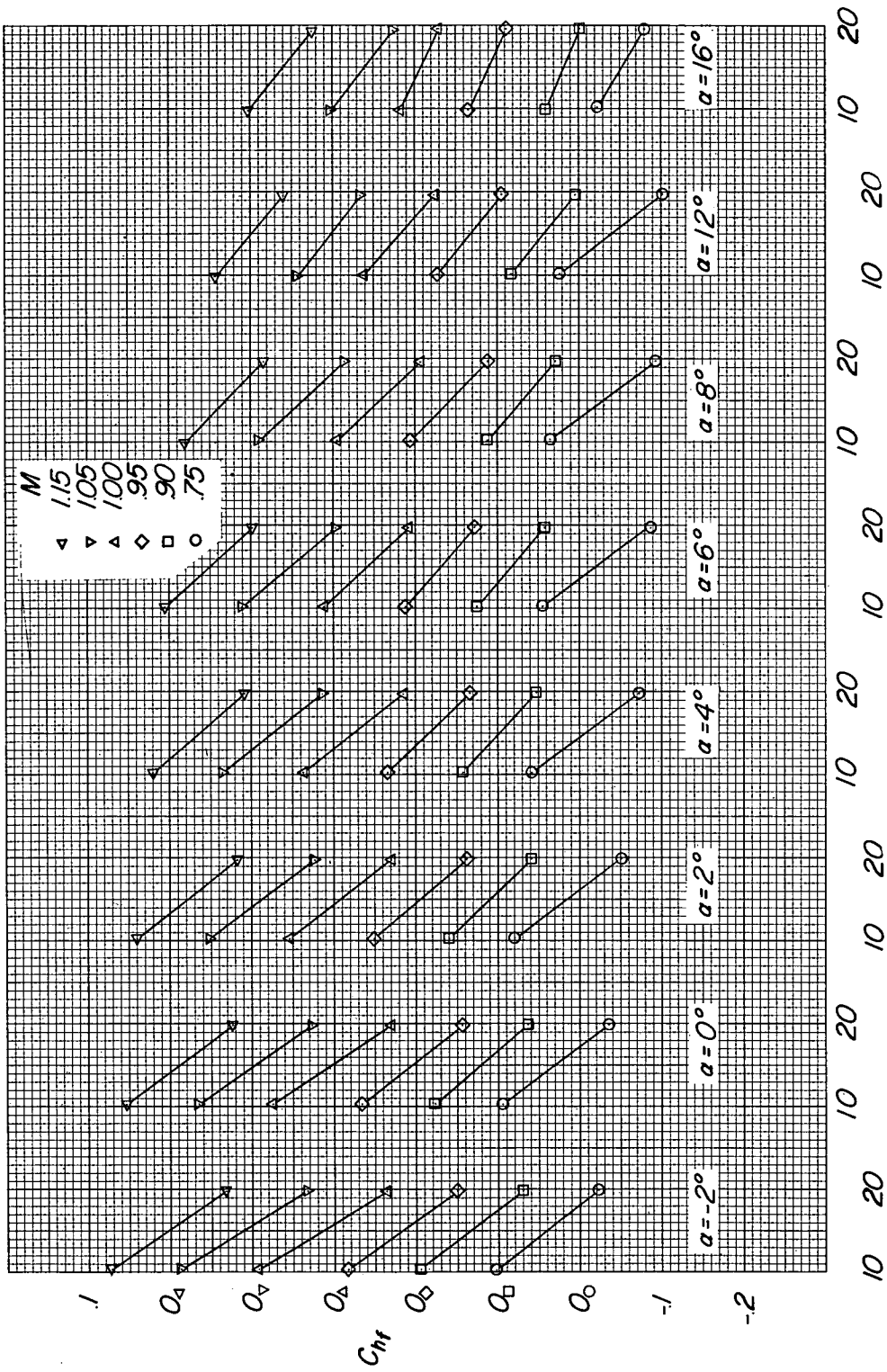

(g) $\delta_t \approx -30.3°$.

Figure 6.- Concluded.

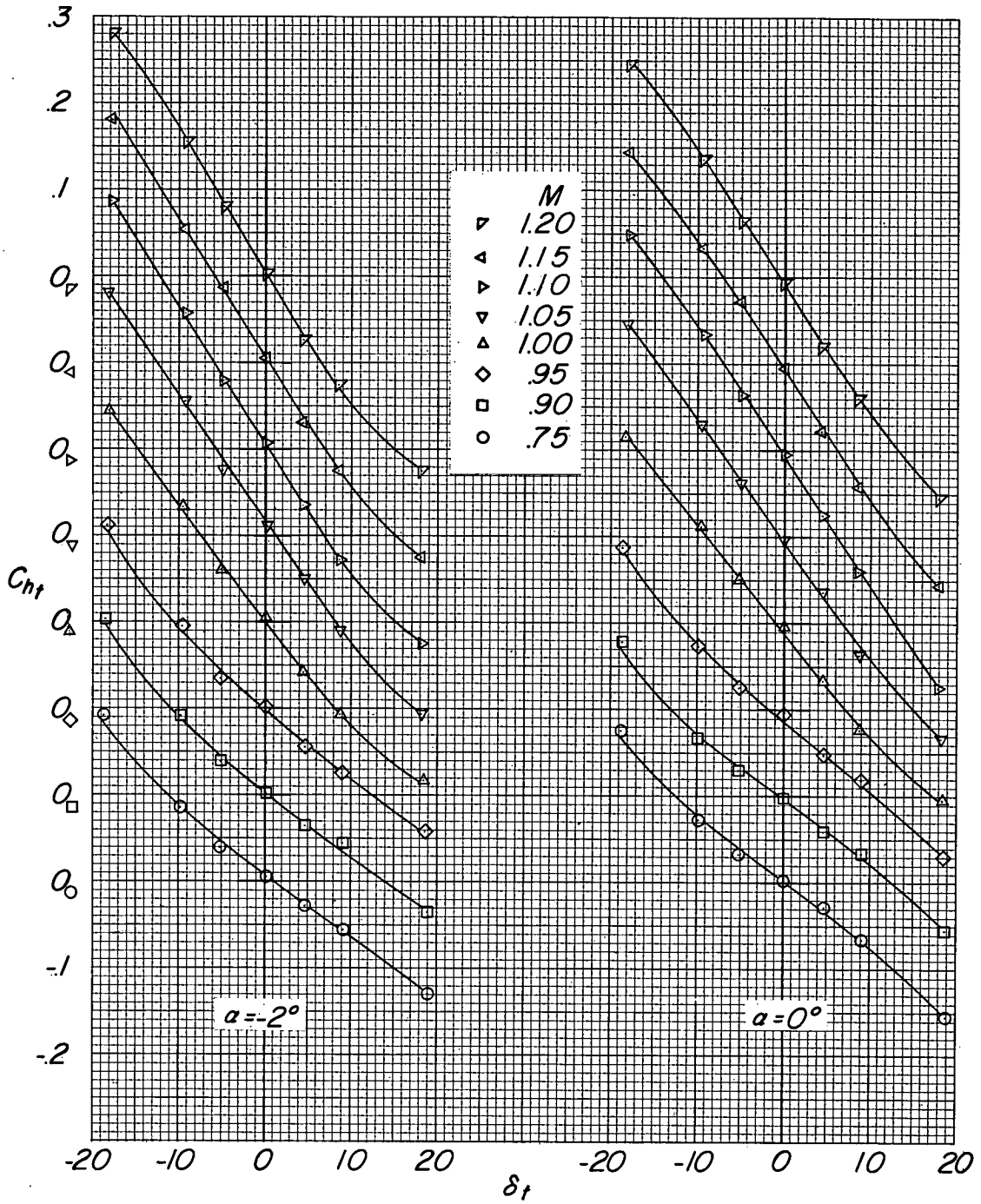

(a) $\delta_f \approx 0°$.

Figure 7.- Variation of tab hinge-moment coefficient with tab deflection for various Mach numbers, angles of attack, and flap deflections.

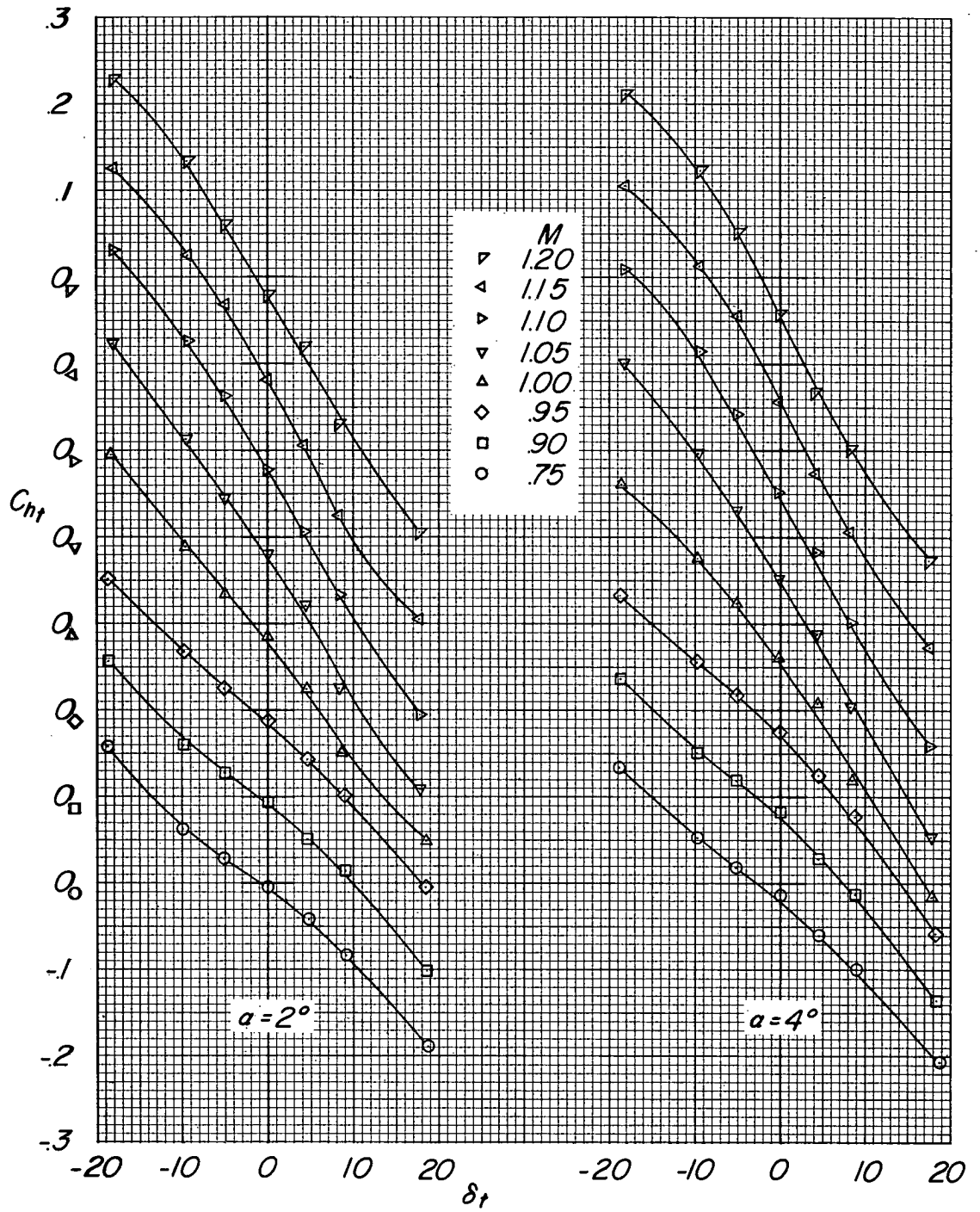

(a) Continued.

Figure 7.- Continued.

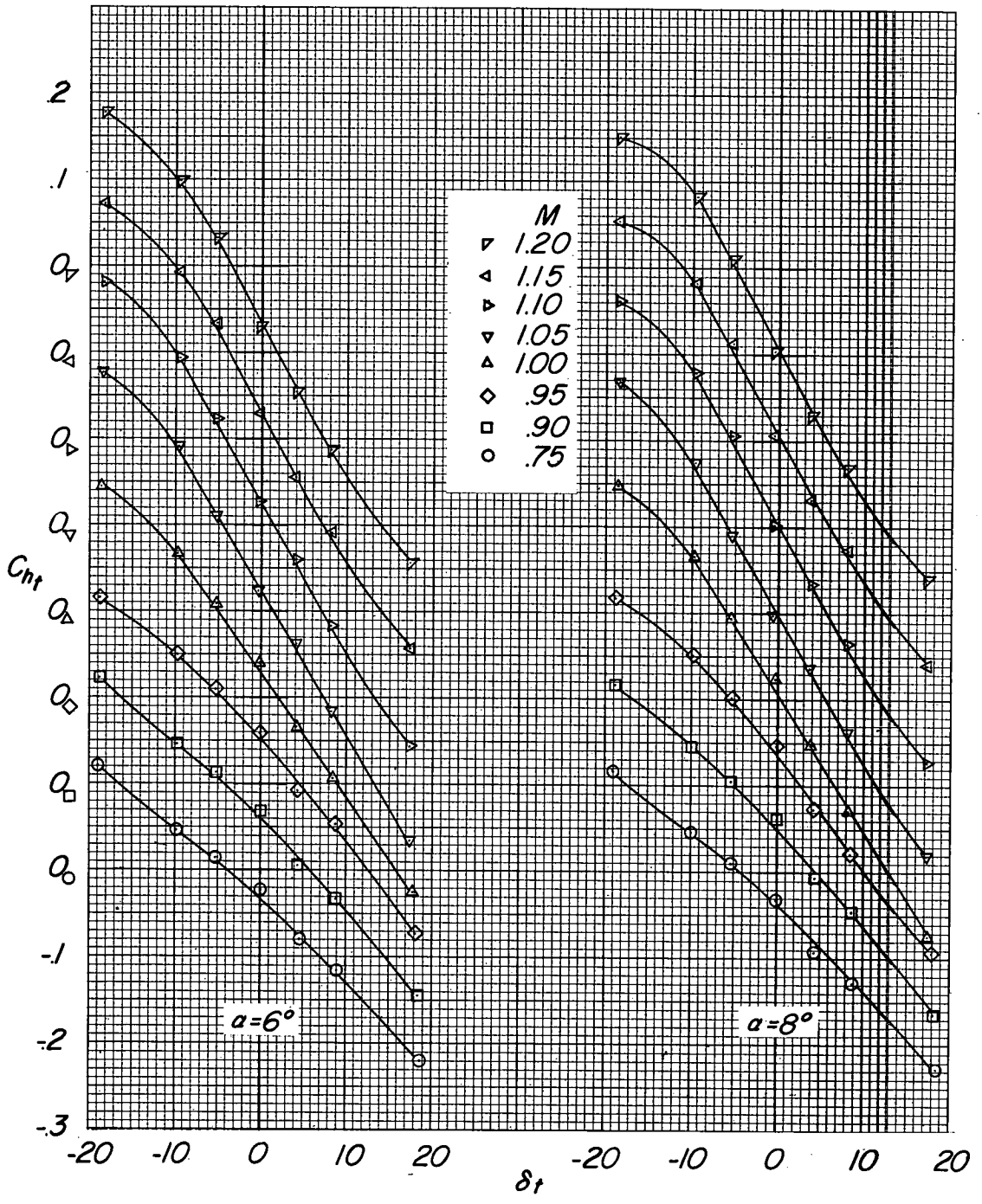

(a) Continued.

Figure 7.- Continued.

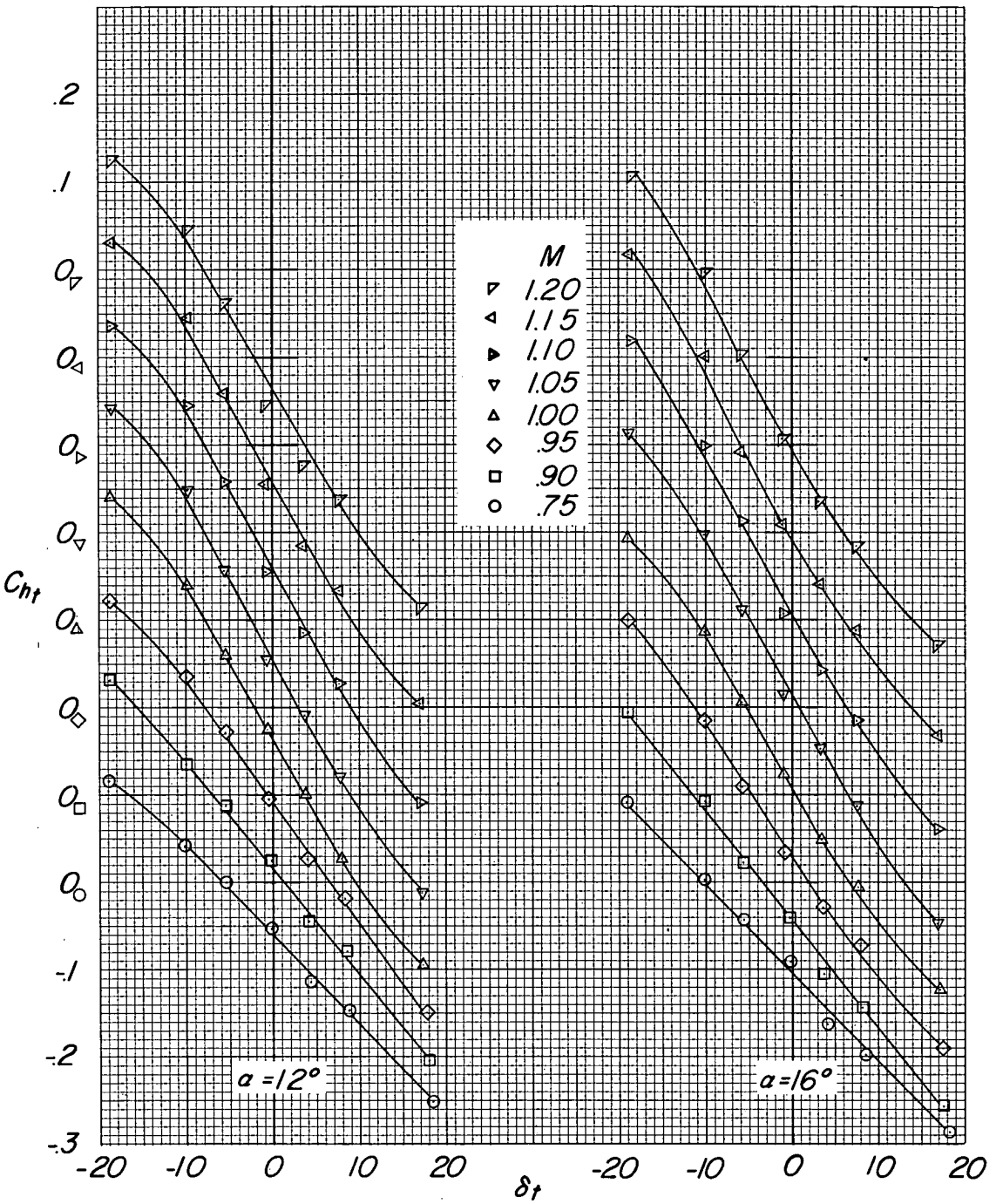

(a) Concluded.

Figure 7.- Continued.

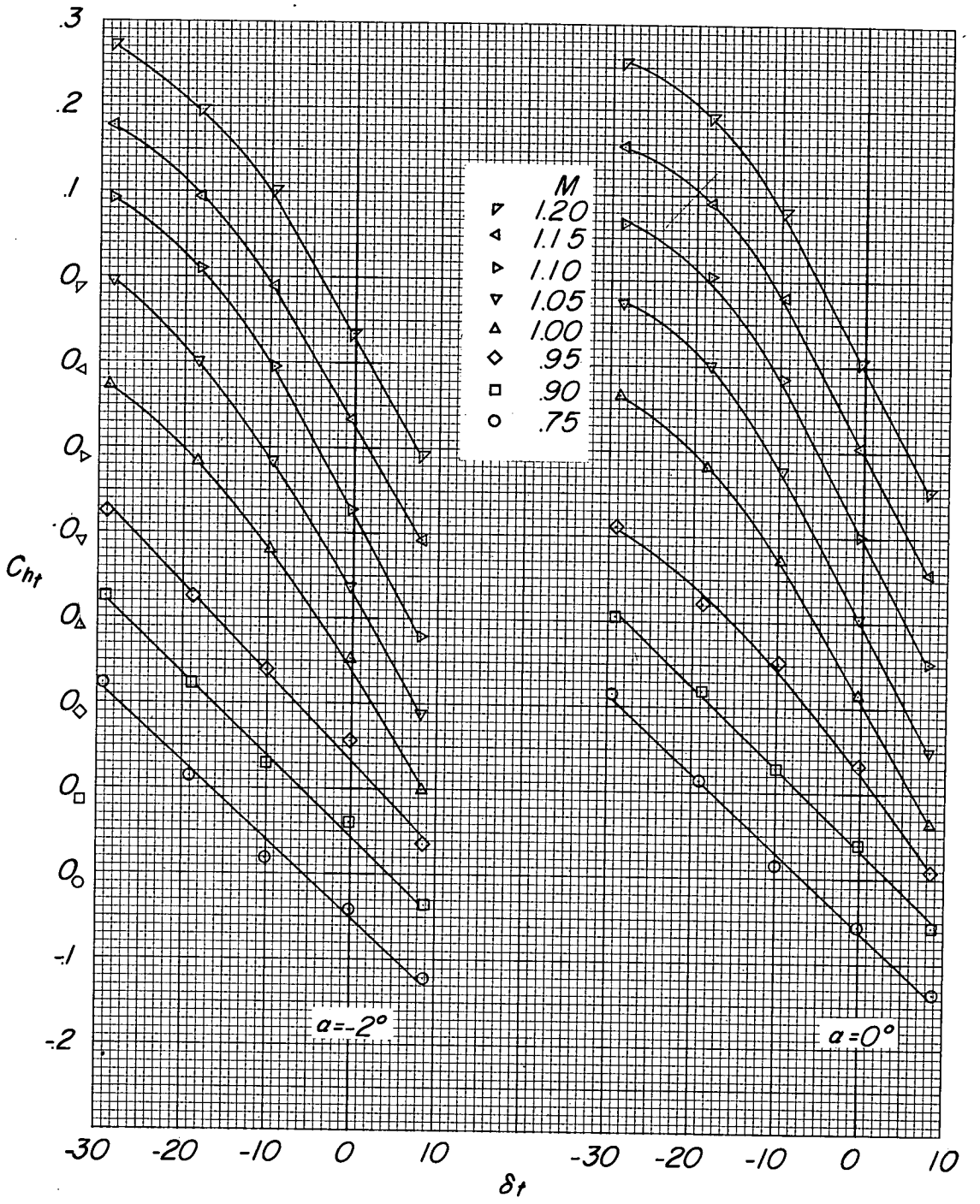

(b) $\delta_f \approx 10.1°$.

Figure 7.- Continued.

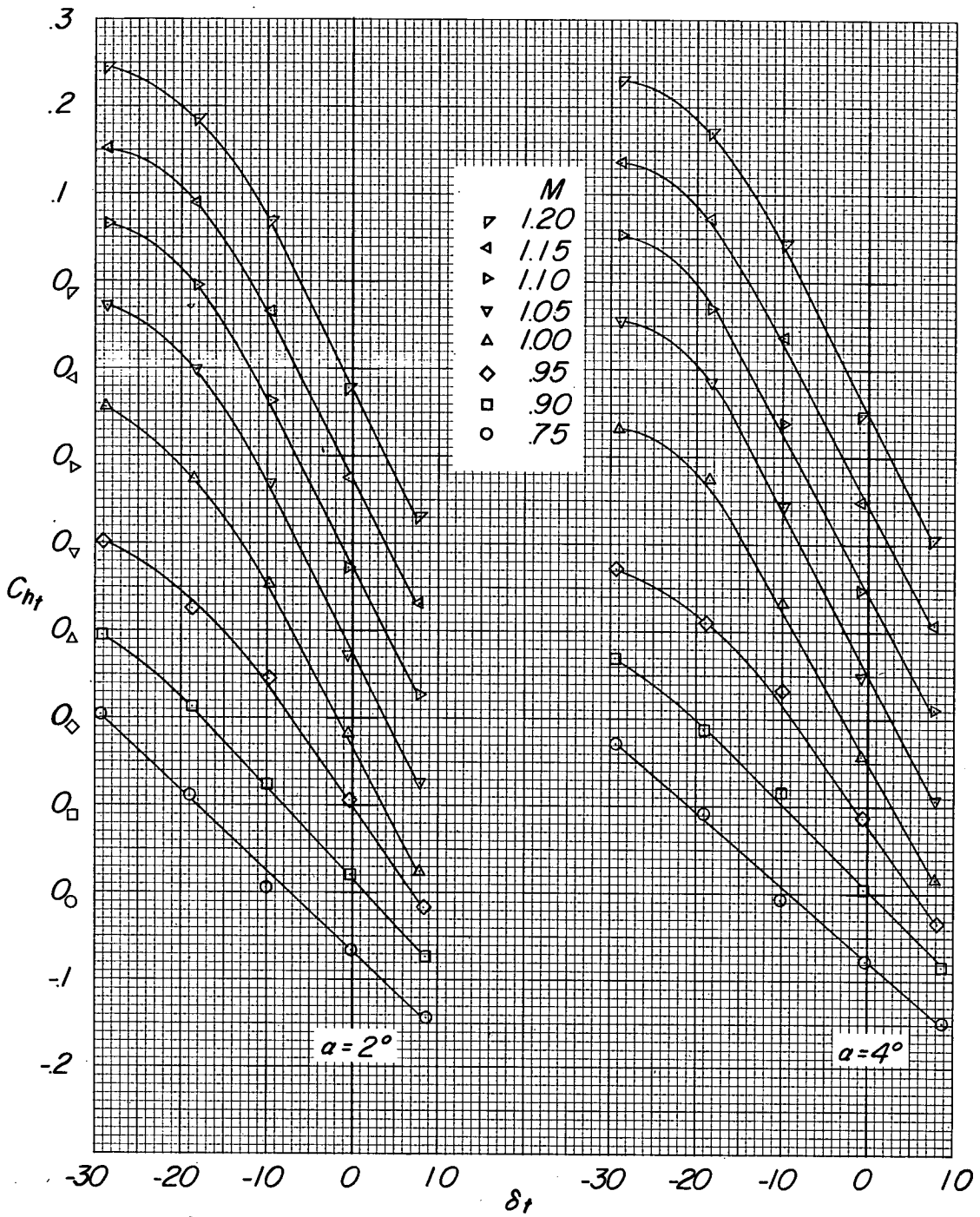

(b) Continued.

Figure 7.- Continued.

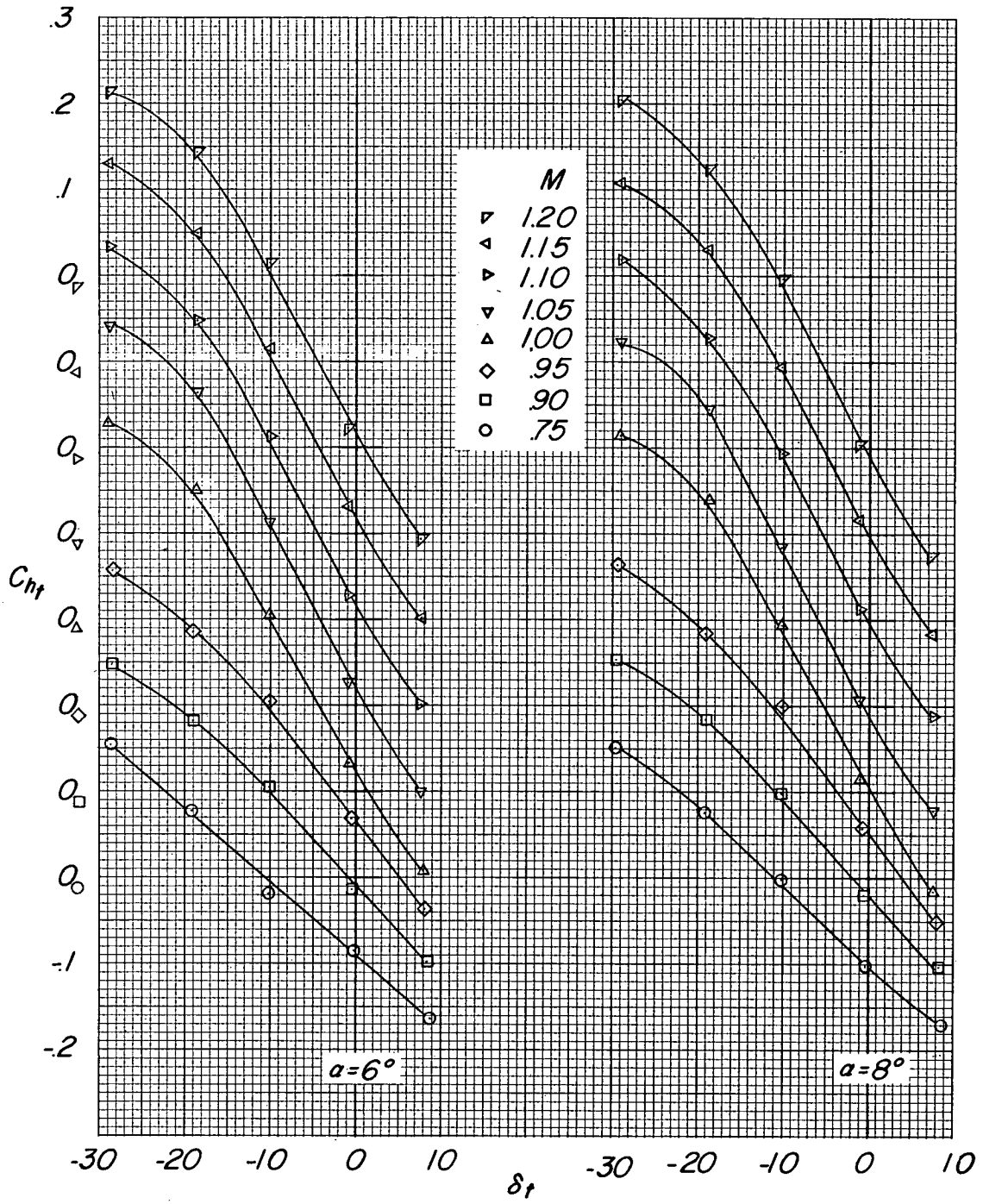

(b) Continued.

Figure 7.- Continued.

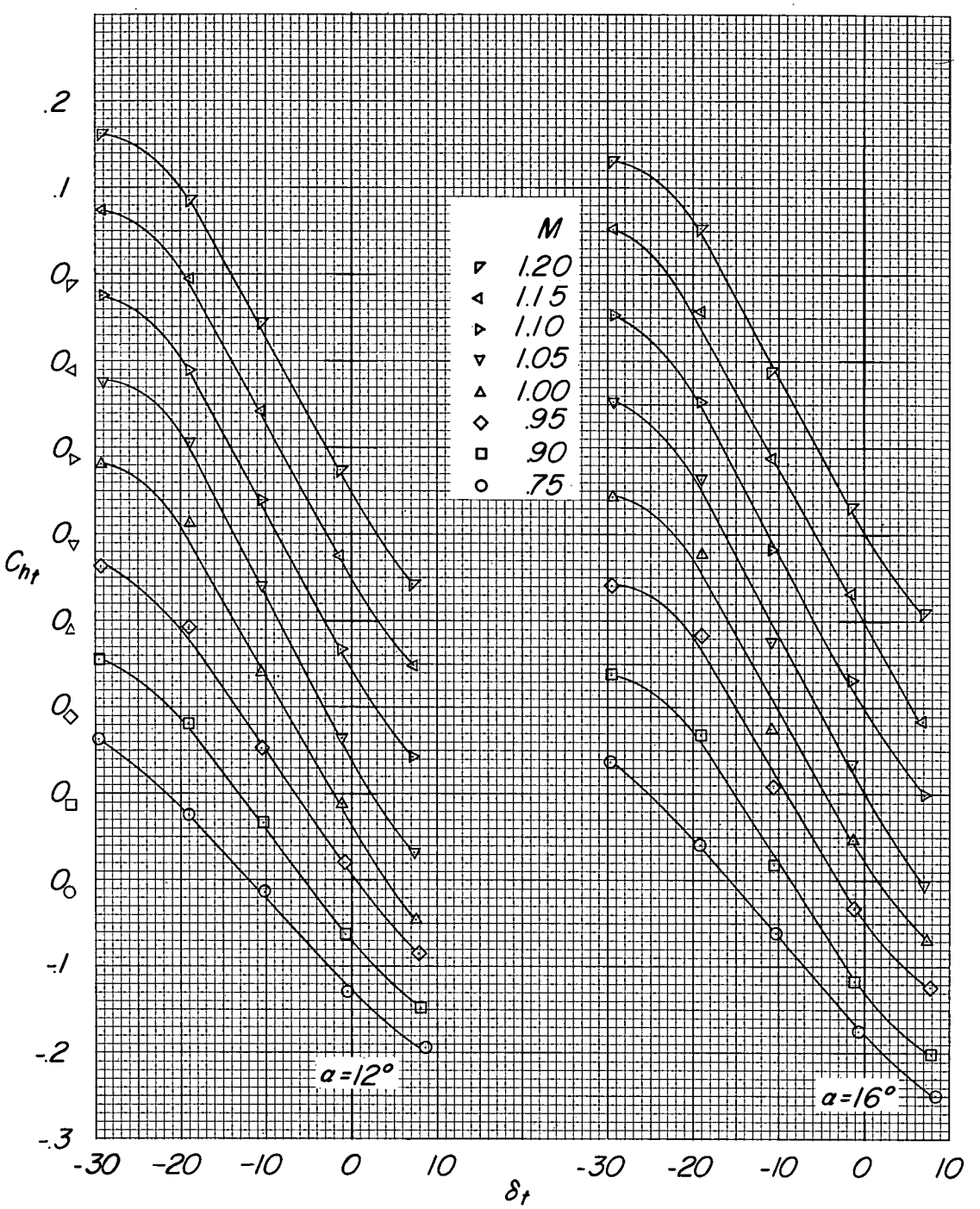

(b) Concluded.

Figure 7.- Continued.

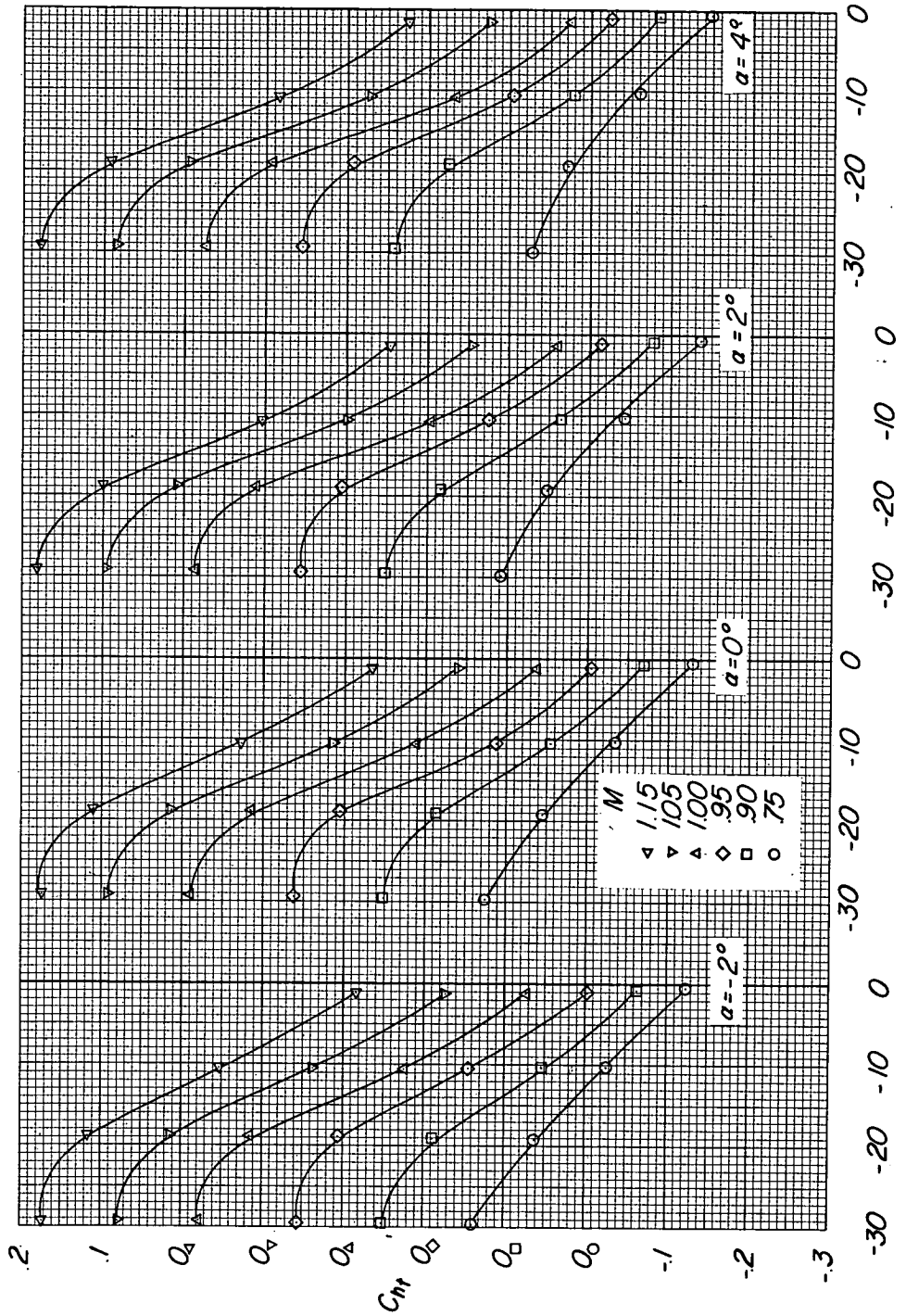

(c) $\delta_f \approx 20°$.

Figure 7.- Continued.

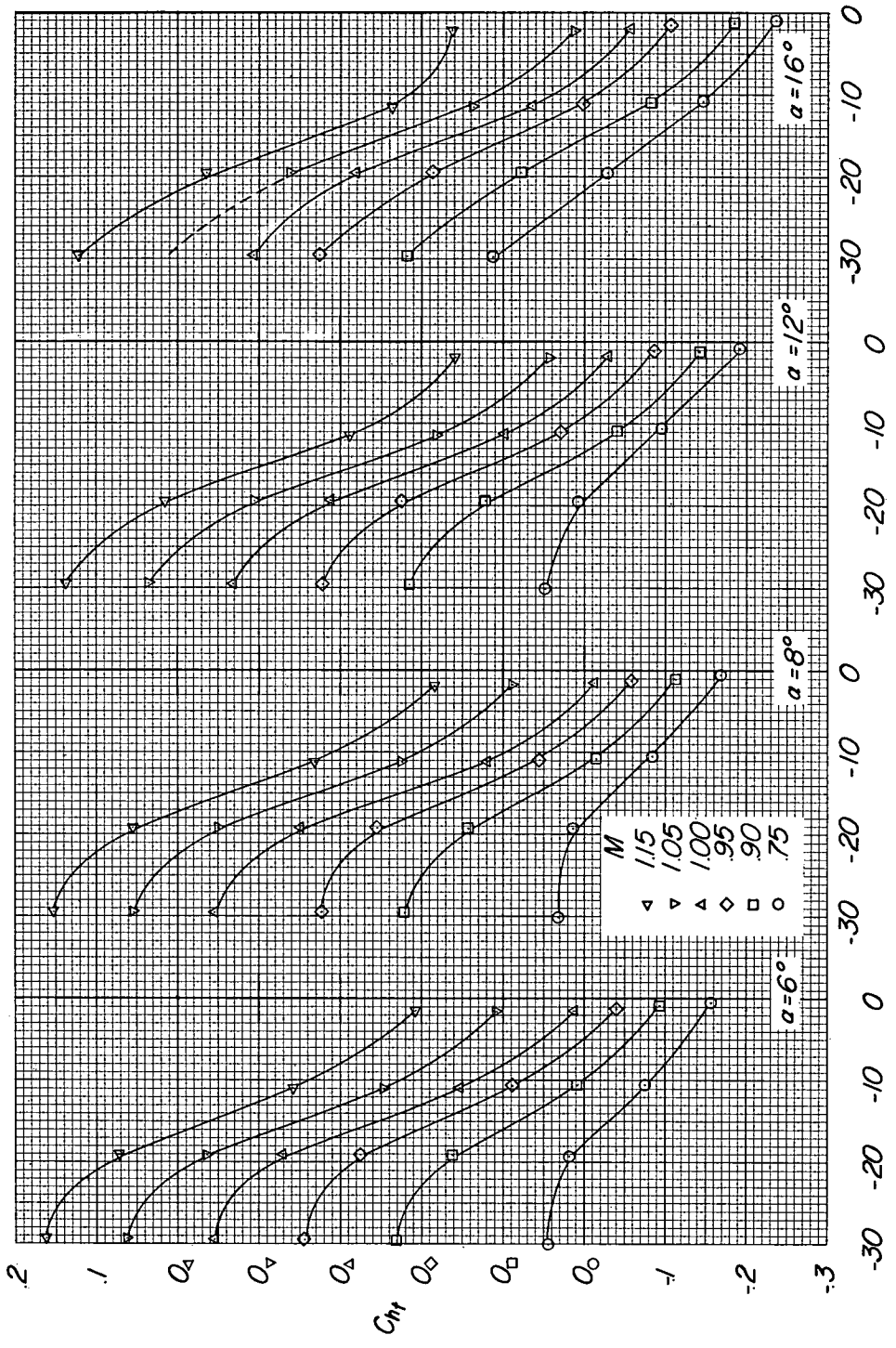

(c) Concluded.

Figure 7.- Continued.

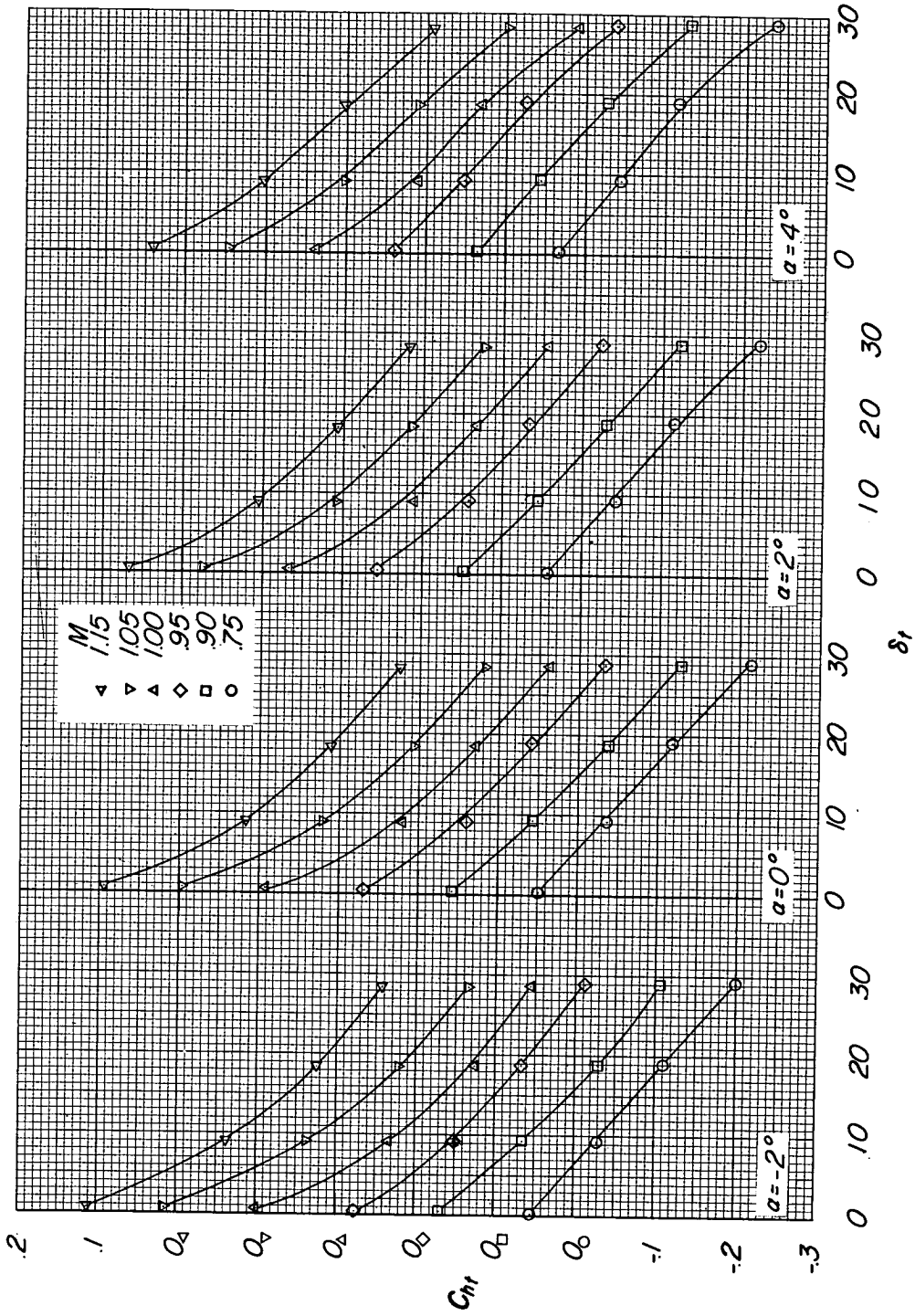

(d) $\delta_f \approx -10.2°$.

Figure 7.- Continued.

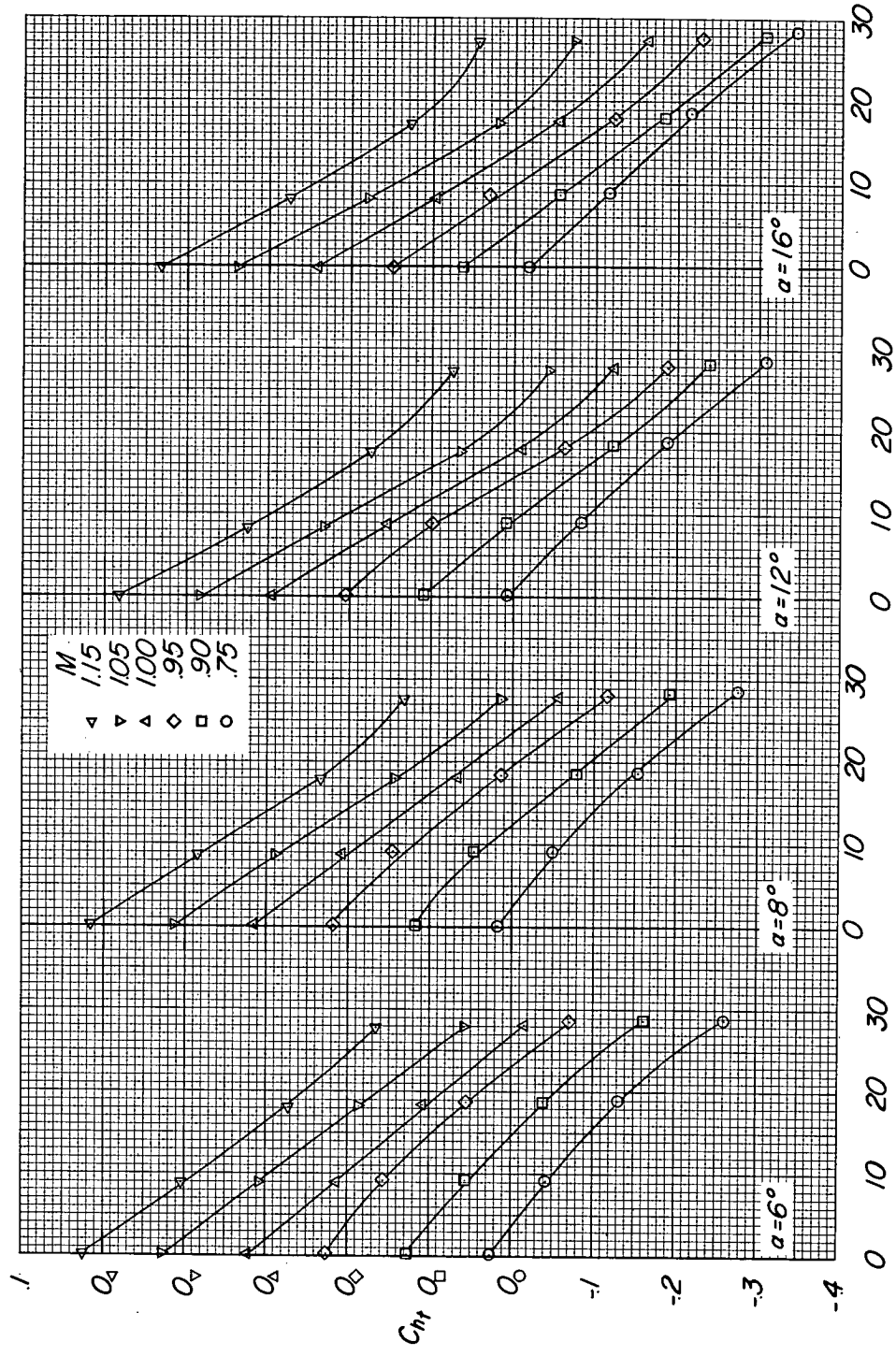

(d) Concluded.

Figure 7.- Continued.

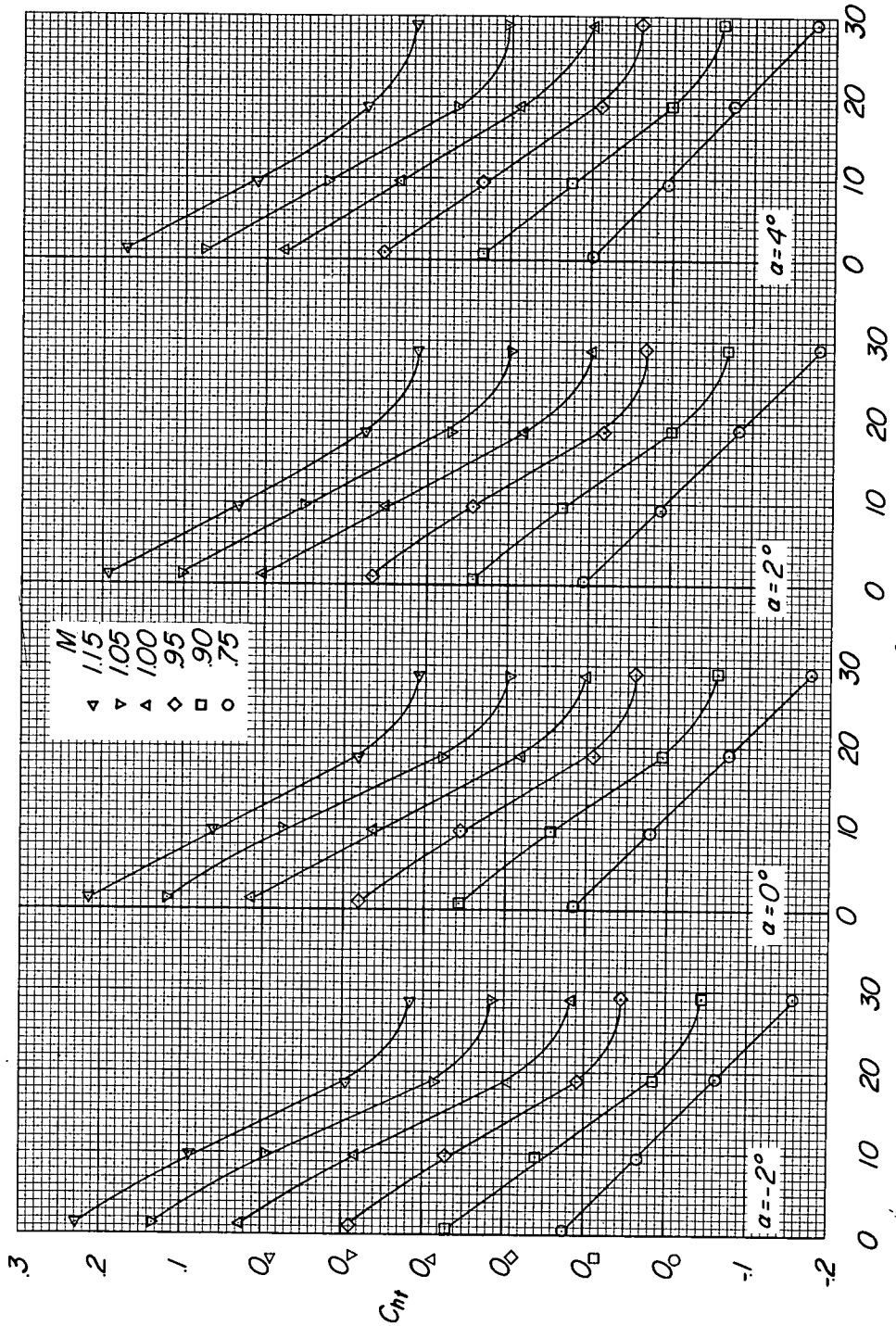

(e) $\delta_f \approx -19.9°$.

Figure 7.- Continued.

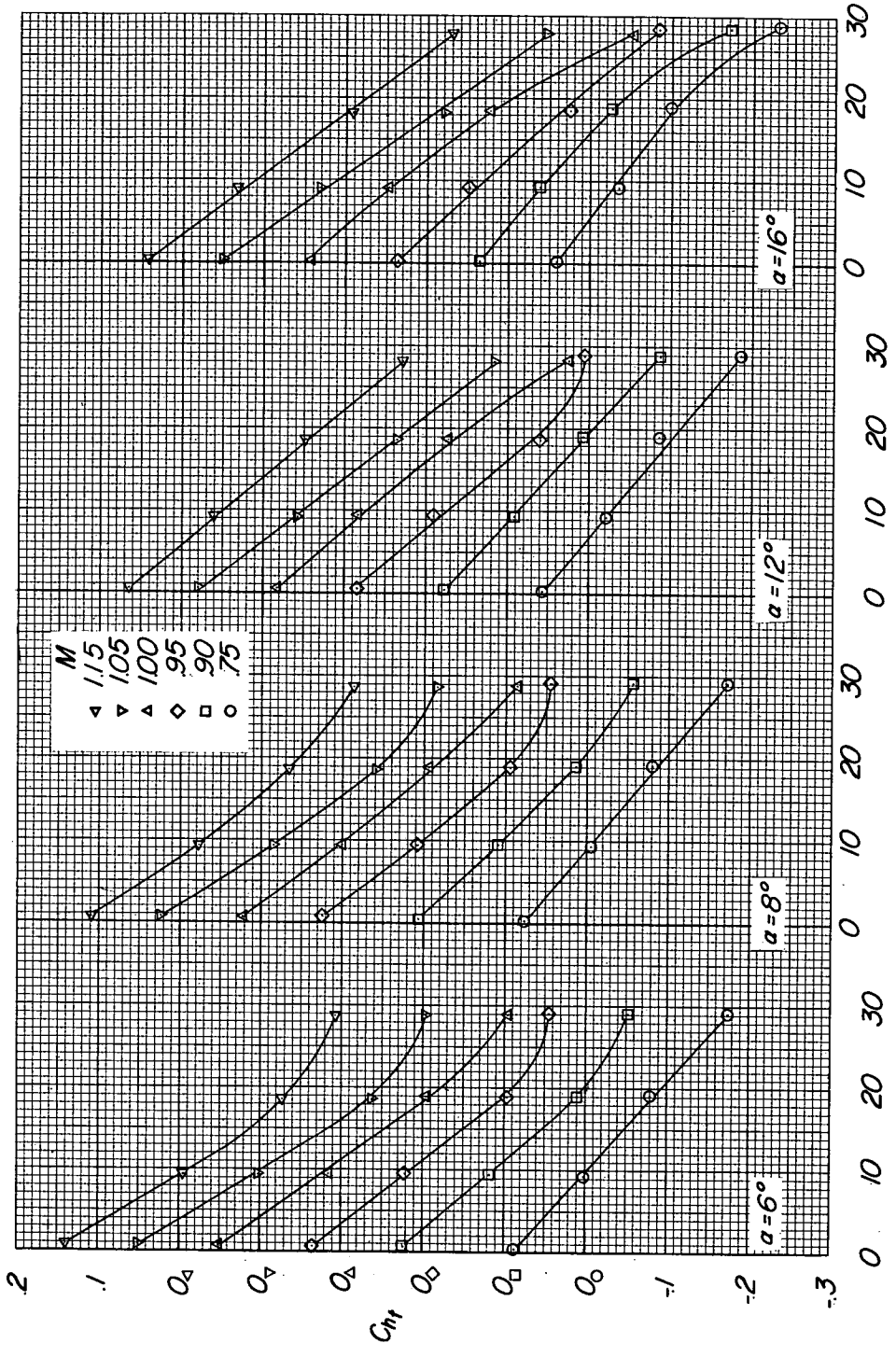

(e) Concluded.

Figure 7.- Concluded.

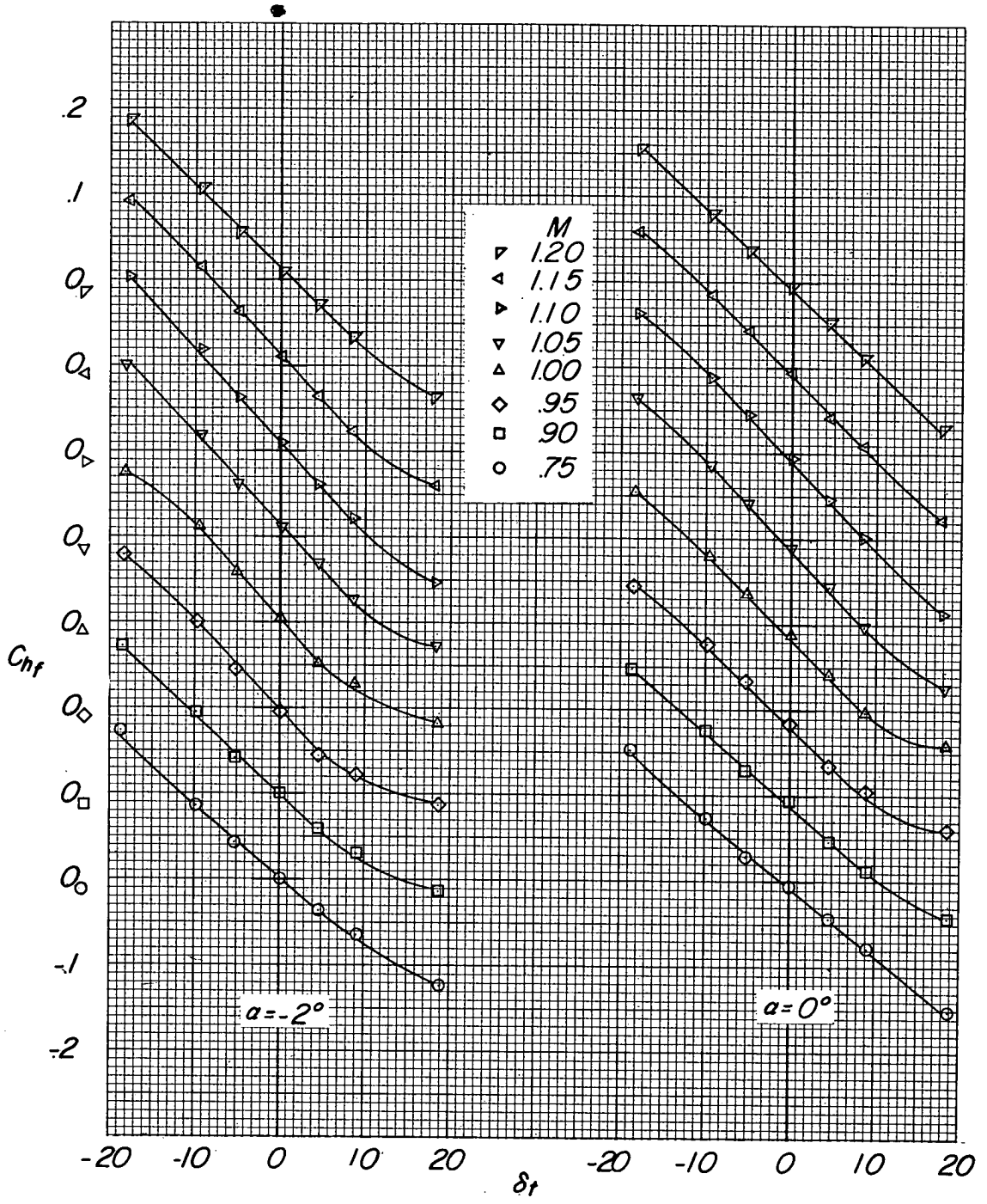

Figure 8.- Variation of flap hinge-moment coefficient with tab deflection for various Mach numbers and angles of attack. $\delta_f \approx 0°$.

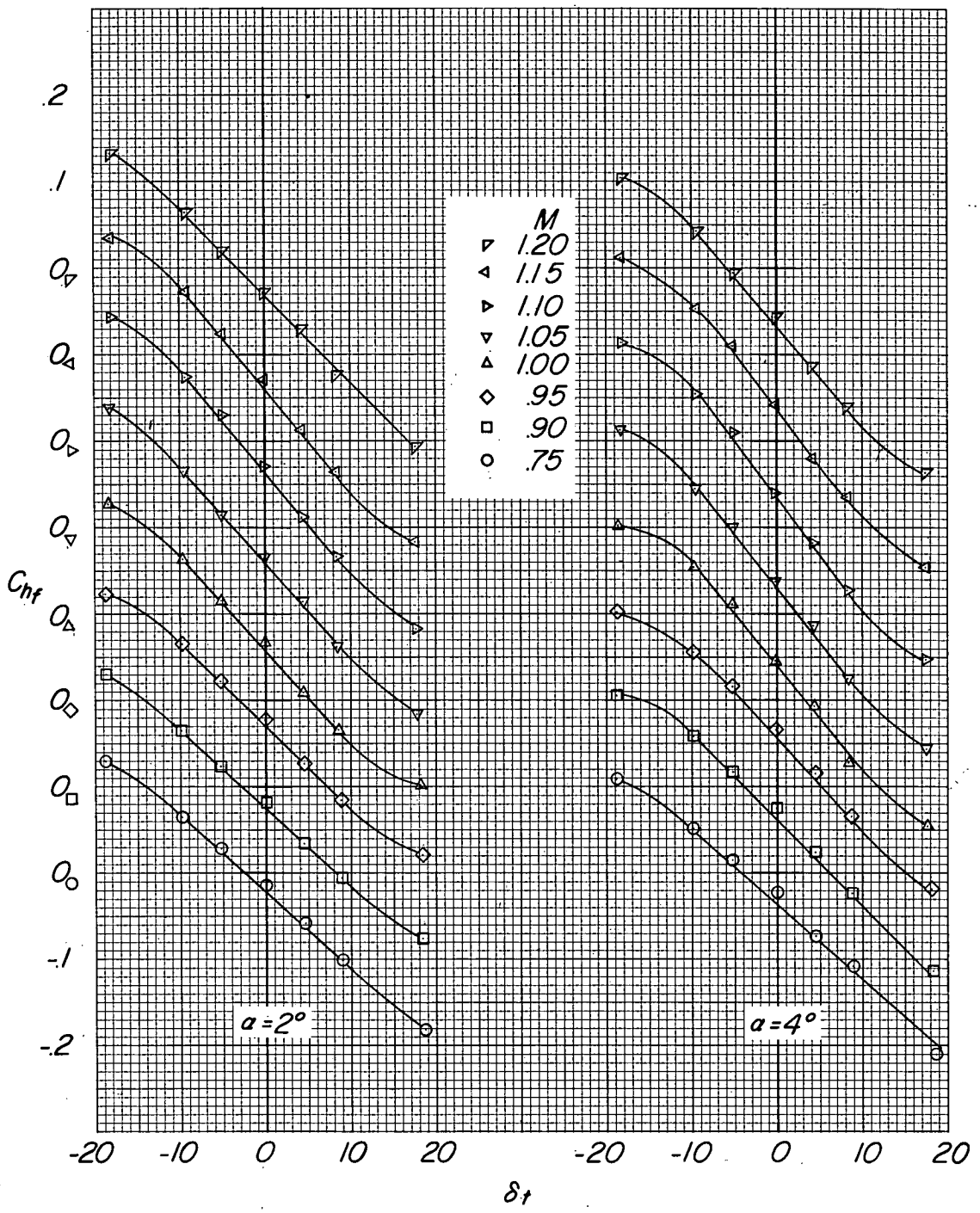

Figure 8.- Continued.

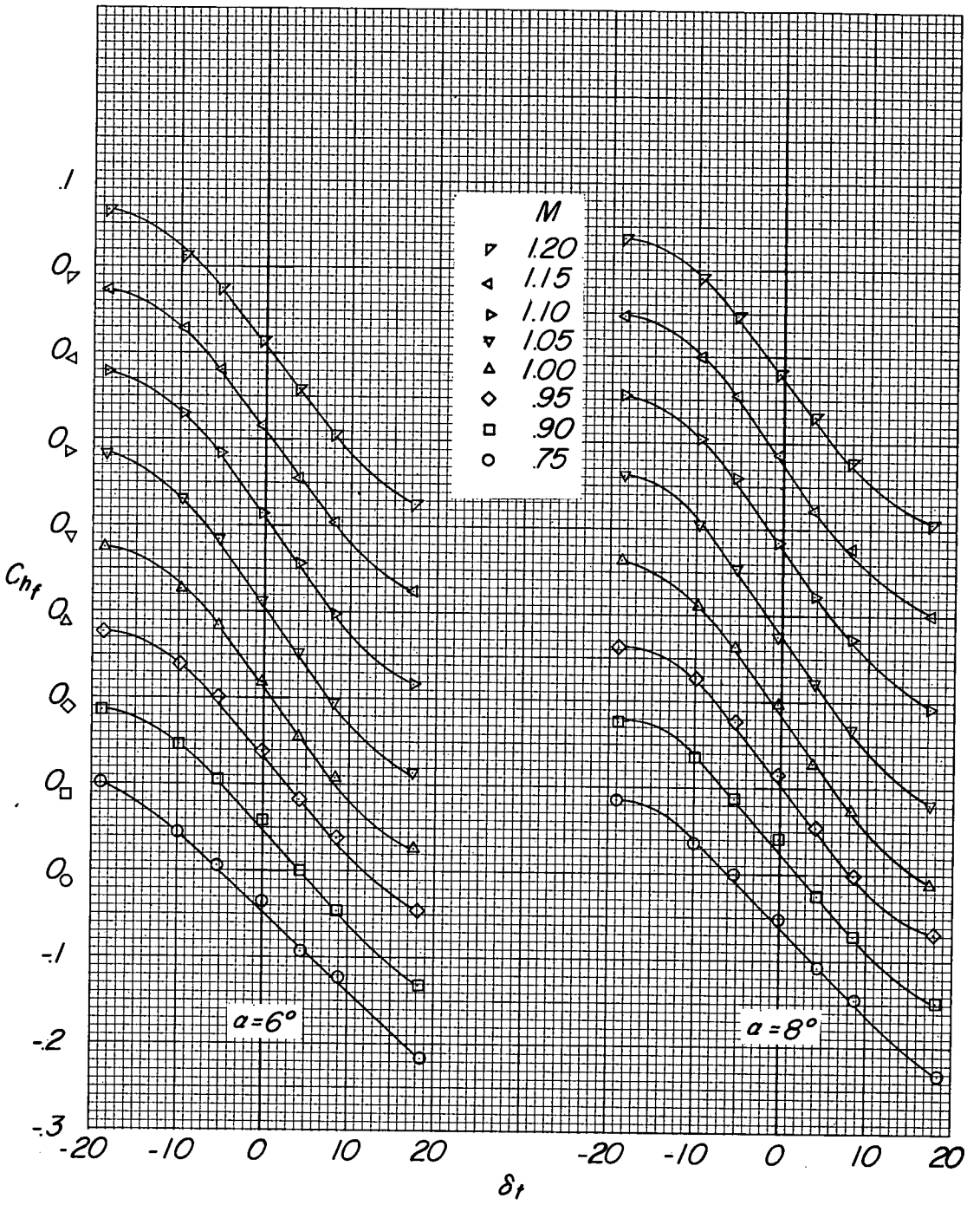

Figure 8.- Continued.

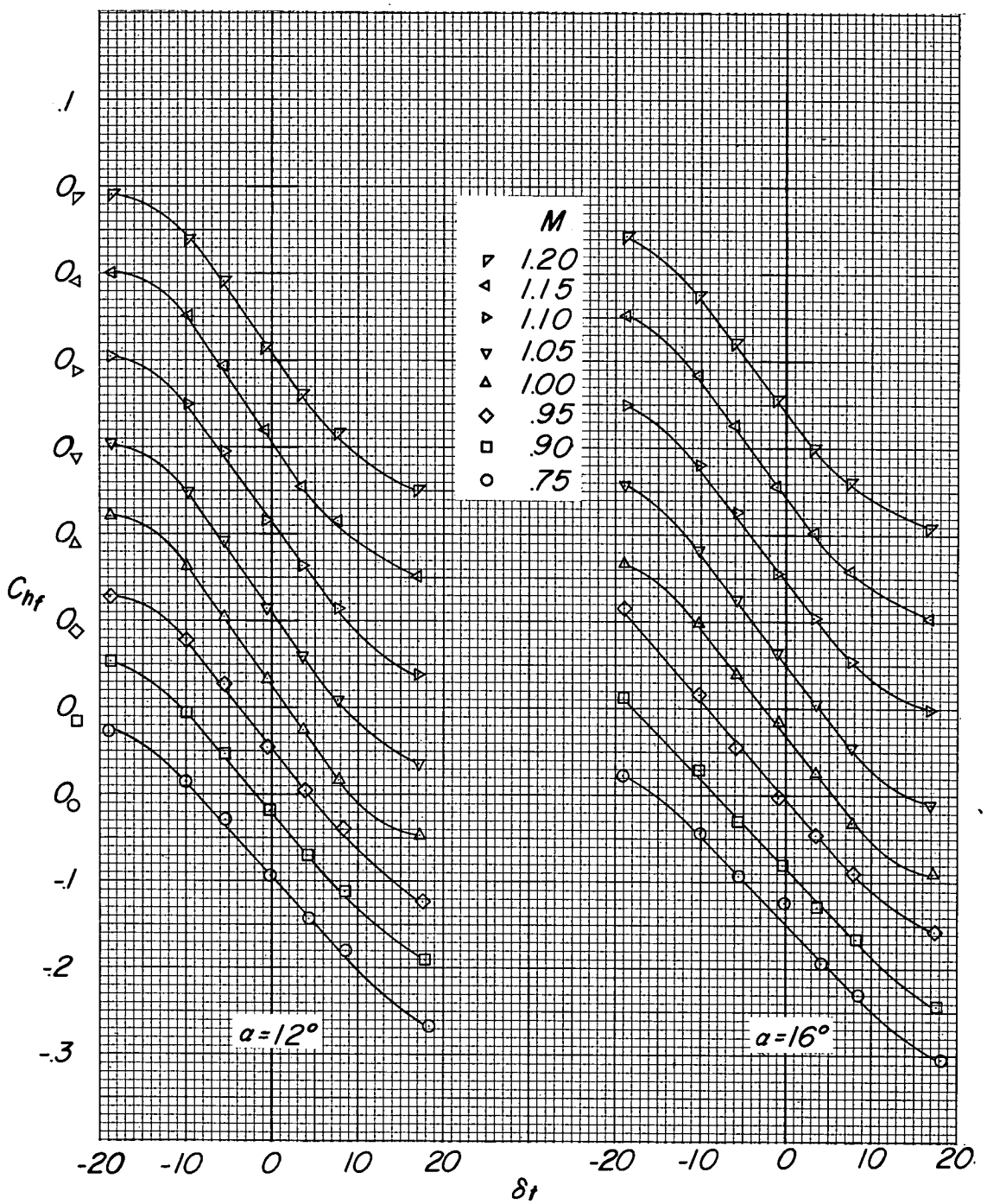

Figure 8.- Concluded.

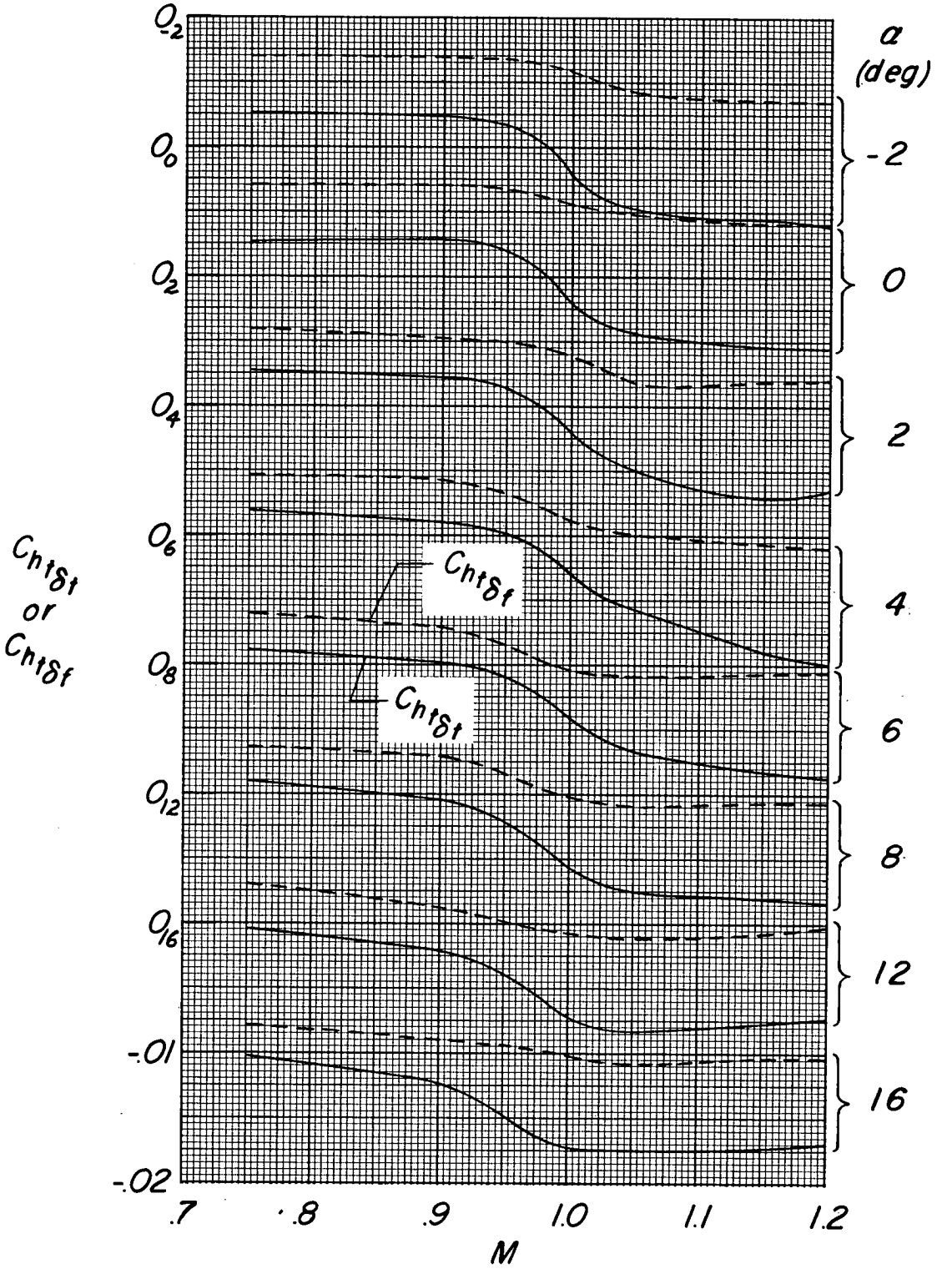

Figure 9.- Variation of tab hinge-moment parameters with Mach number for various angles of attack.

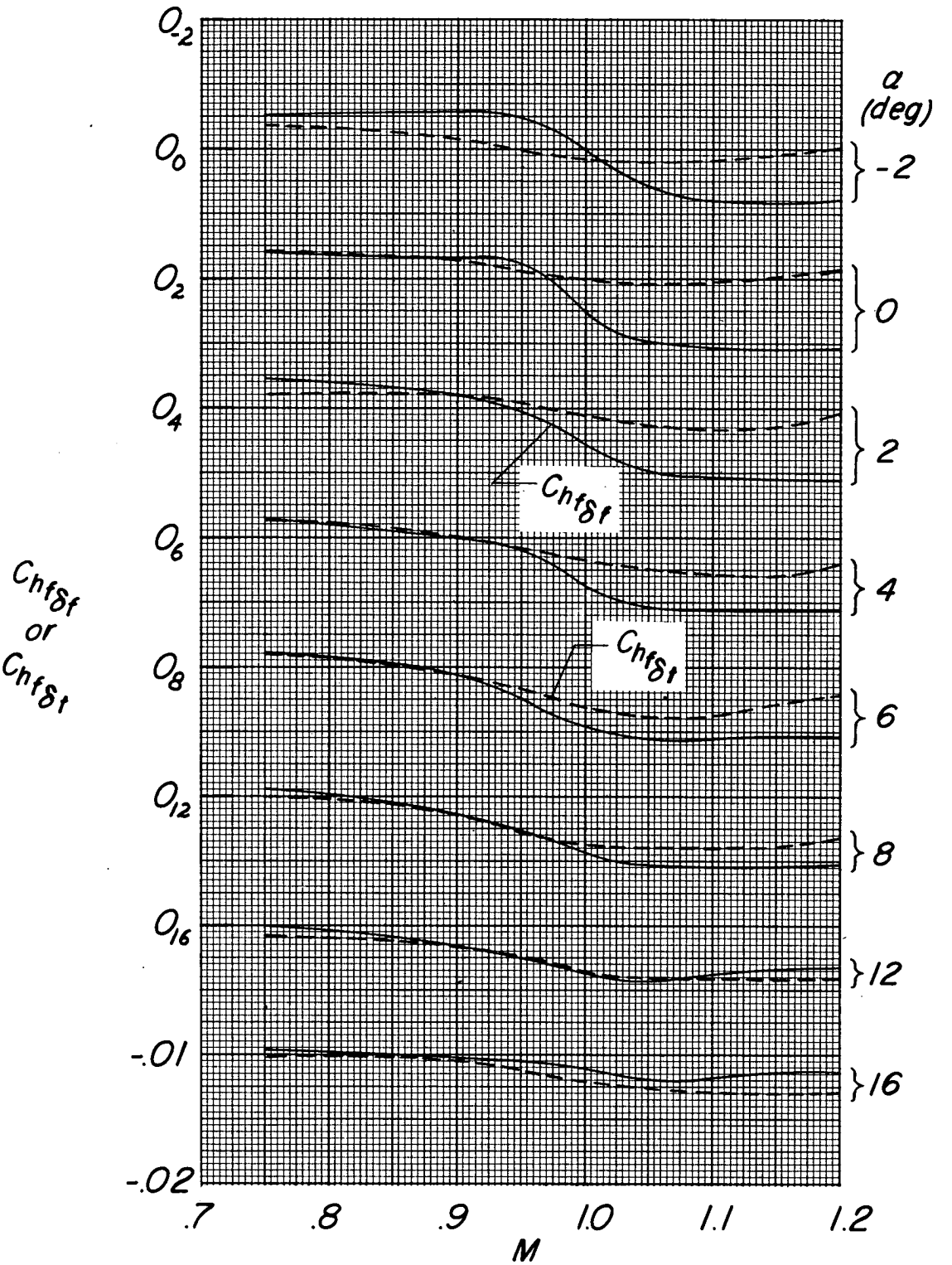

Figure 10.- Variation of flap hinge-moment parameters with Mach number for various angles of attack.

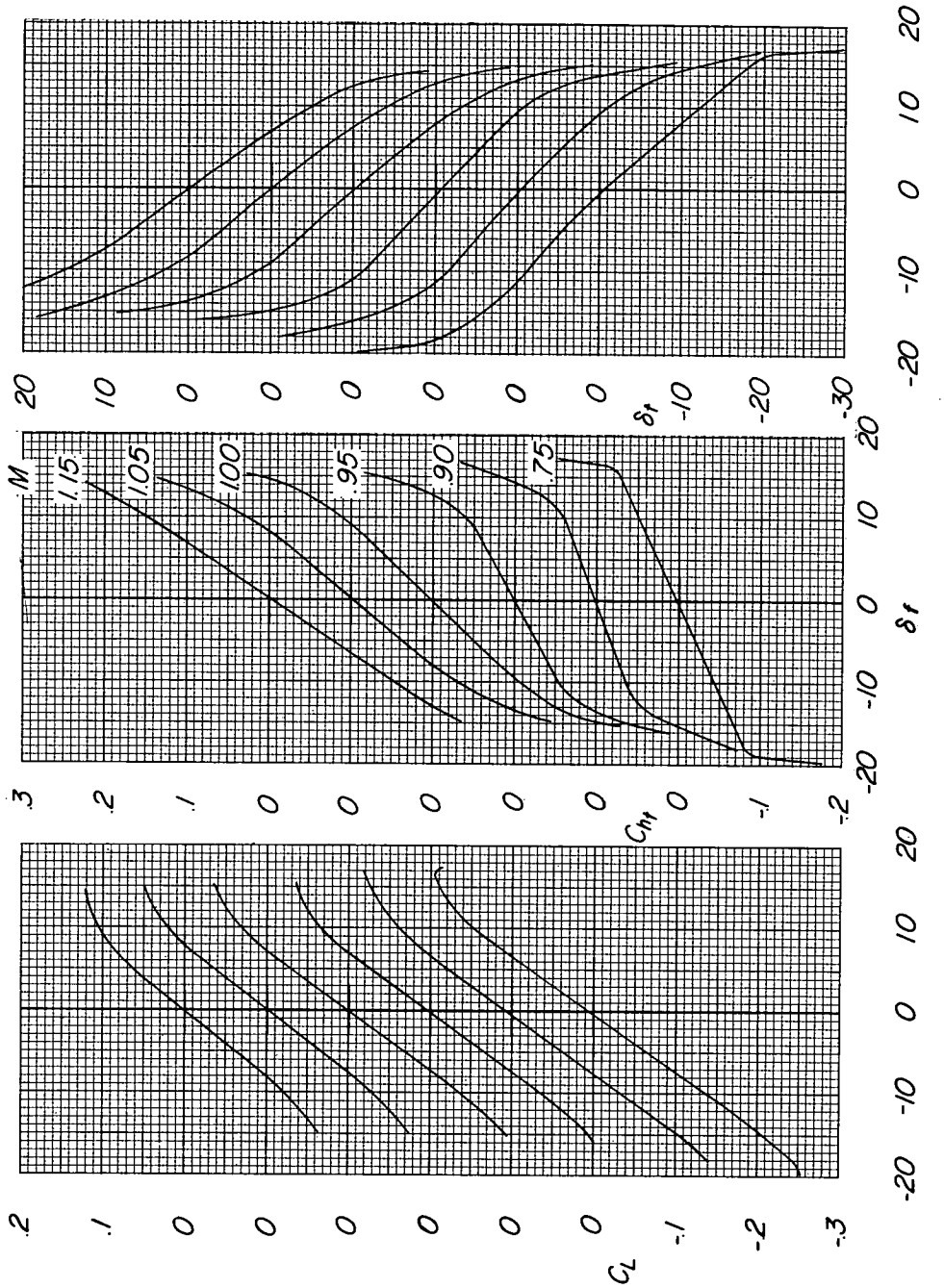

Figure 11.- Variation of lift coefficient, tab hinge-moment coefficient, and tab deflection with flap deflection under conditions for which $\Delta C_{h_f} = 0$ and $\alpha = 0°$.

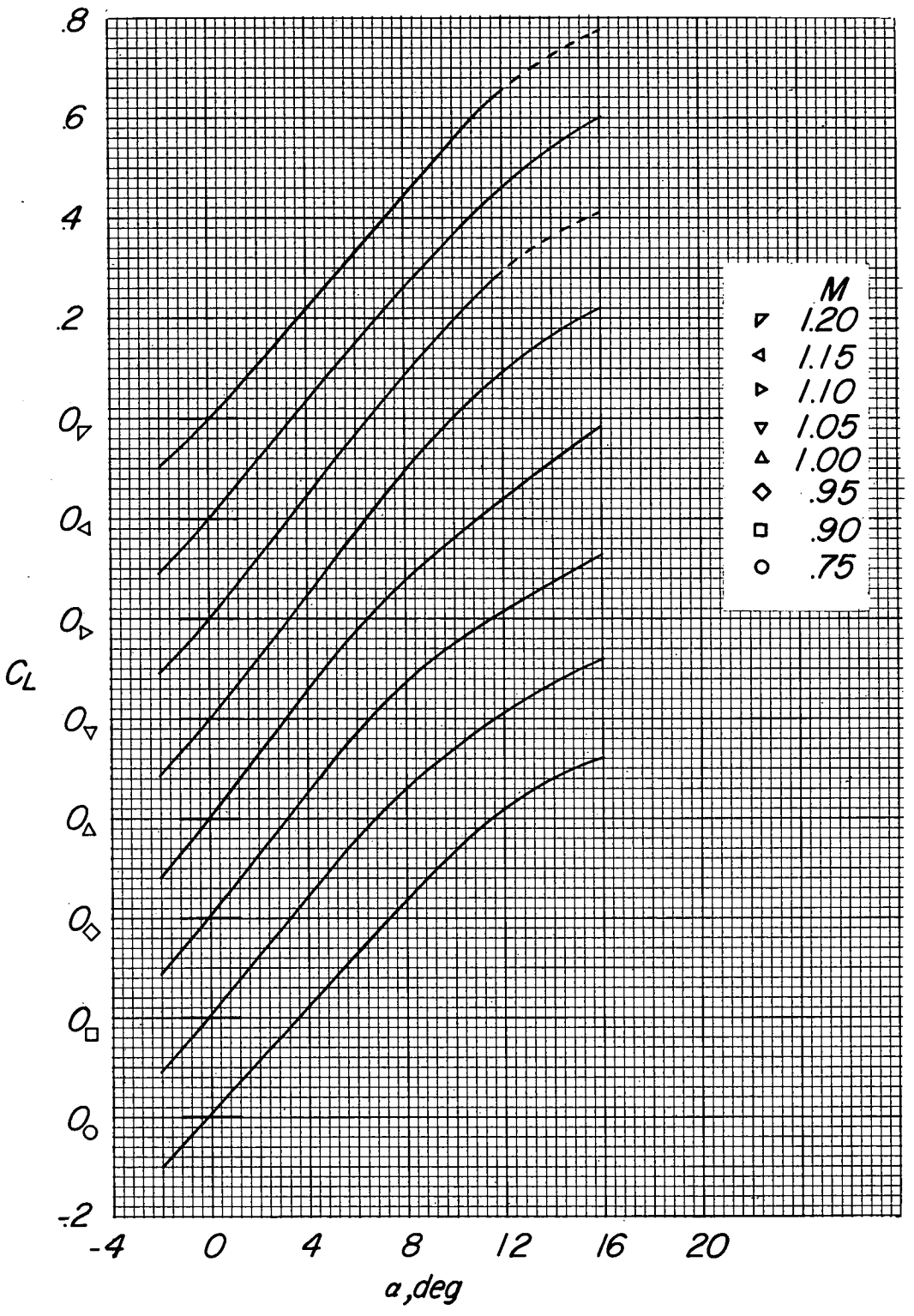

Figure 12.- Lift-coefficient variation with angle of attack for various Mach numbers. $\delta_f \approx 0^\circ$; $\delta_t \approx 0^\circ$.

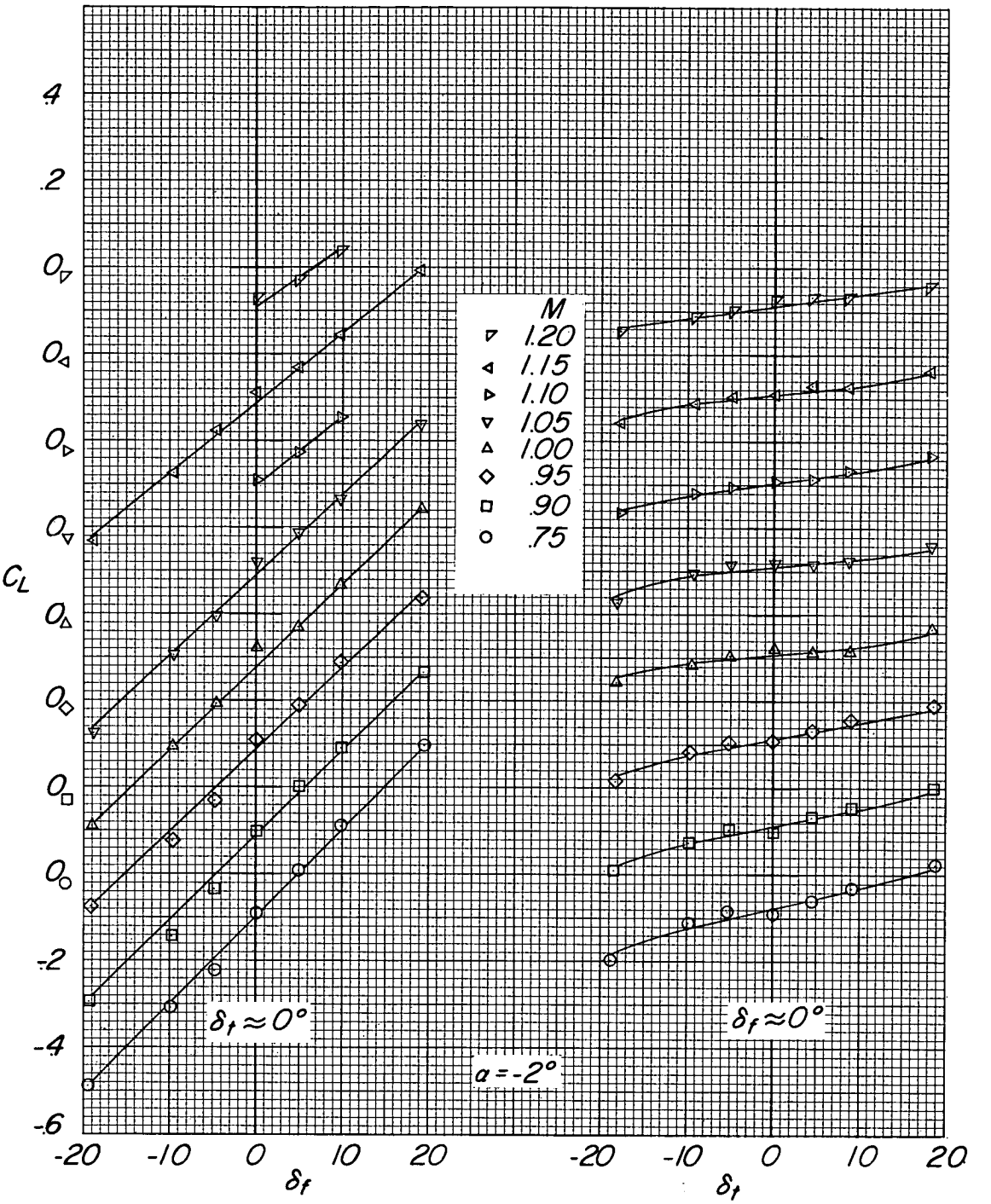

Figure 13.- Variation of lift coefficient with flap deflection and with tab deflection for various Mach numbers and angles of attack.

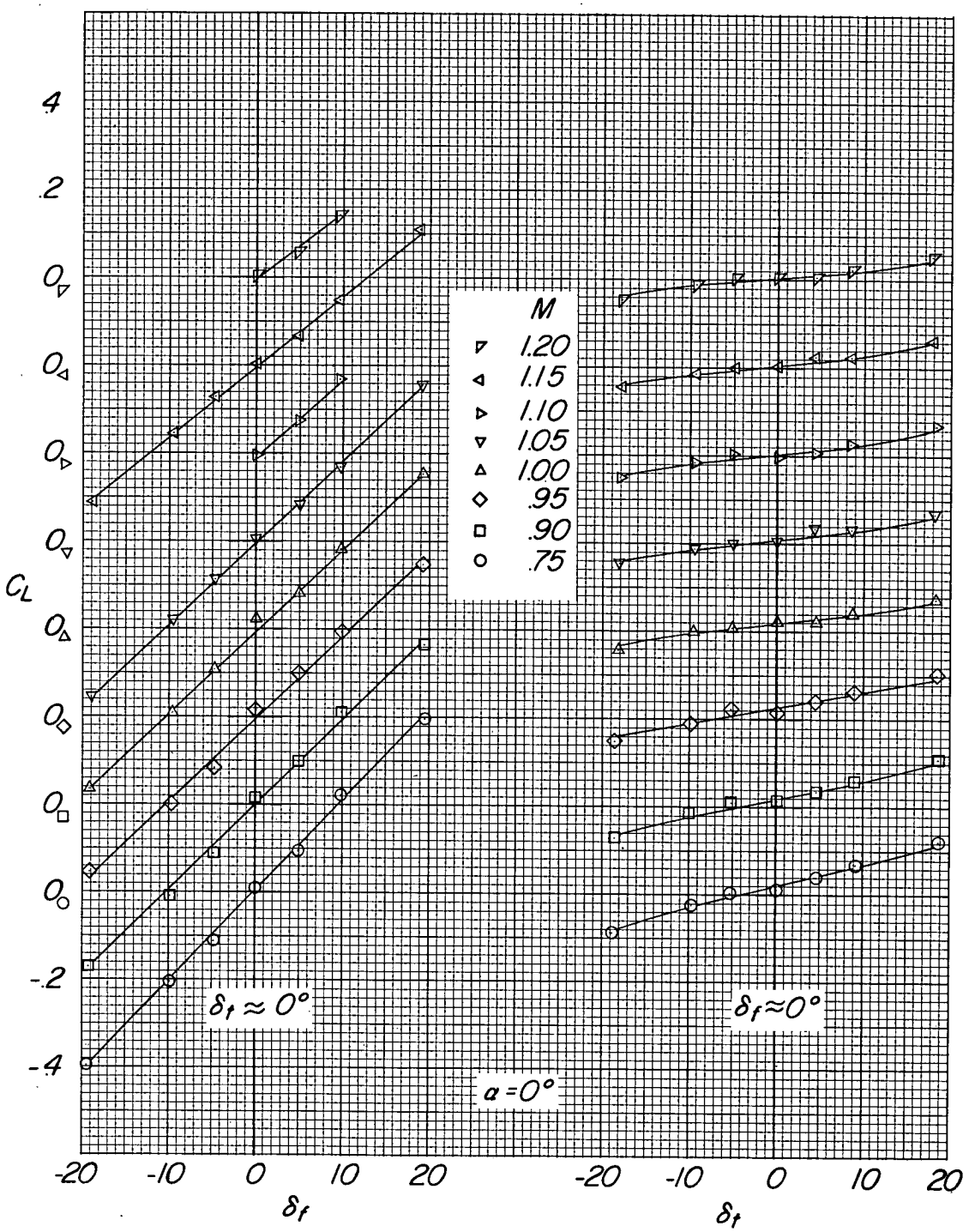

Figure 13.- Continued.

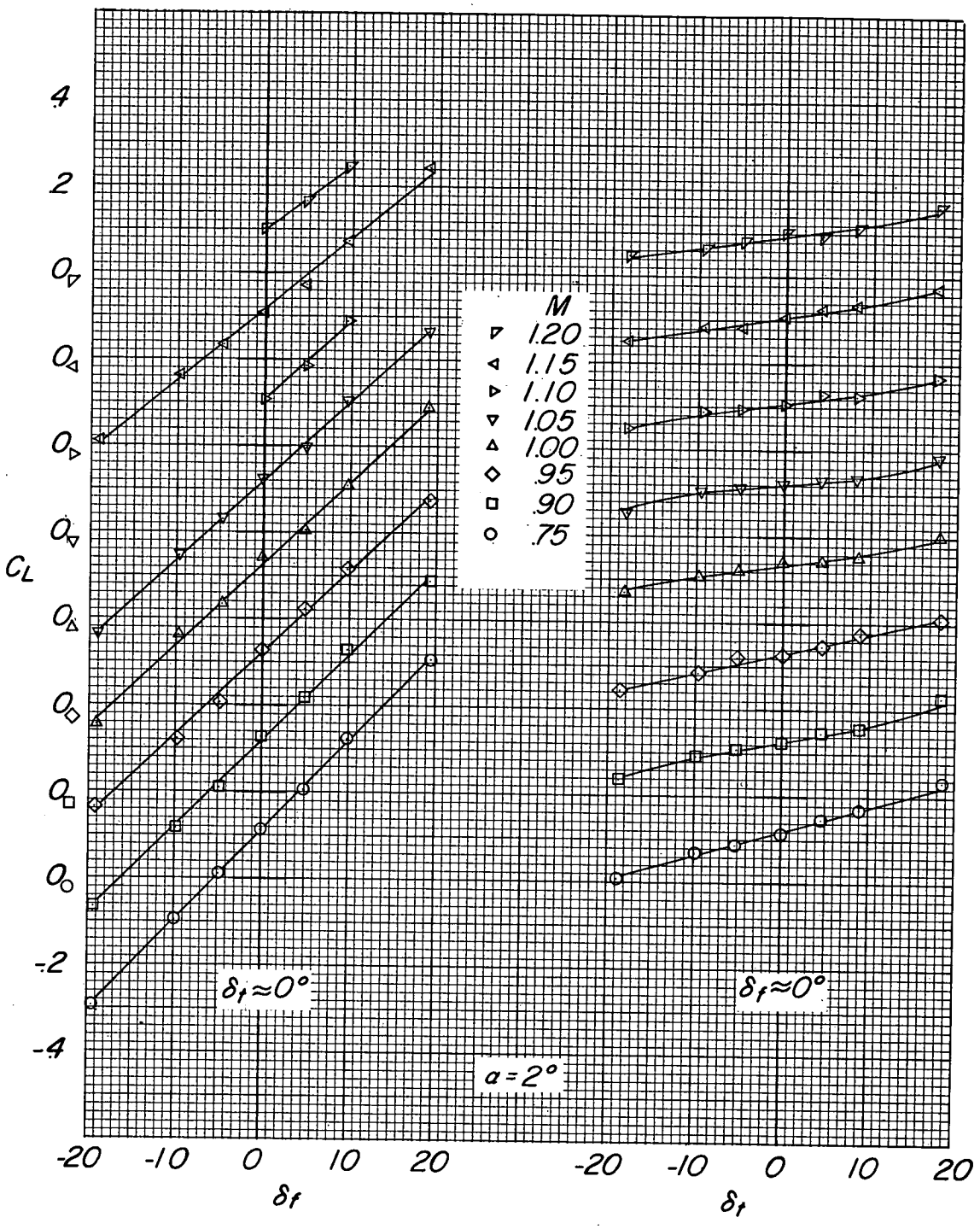

Figure 13.- Continued.

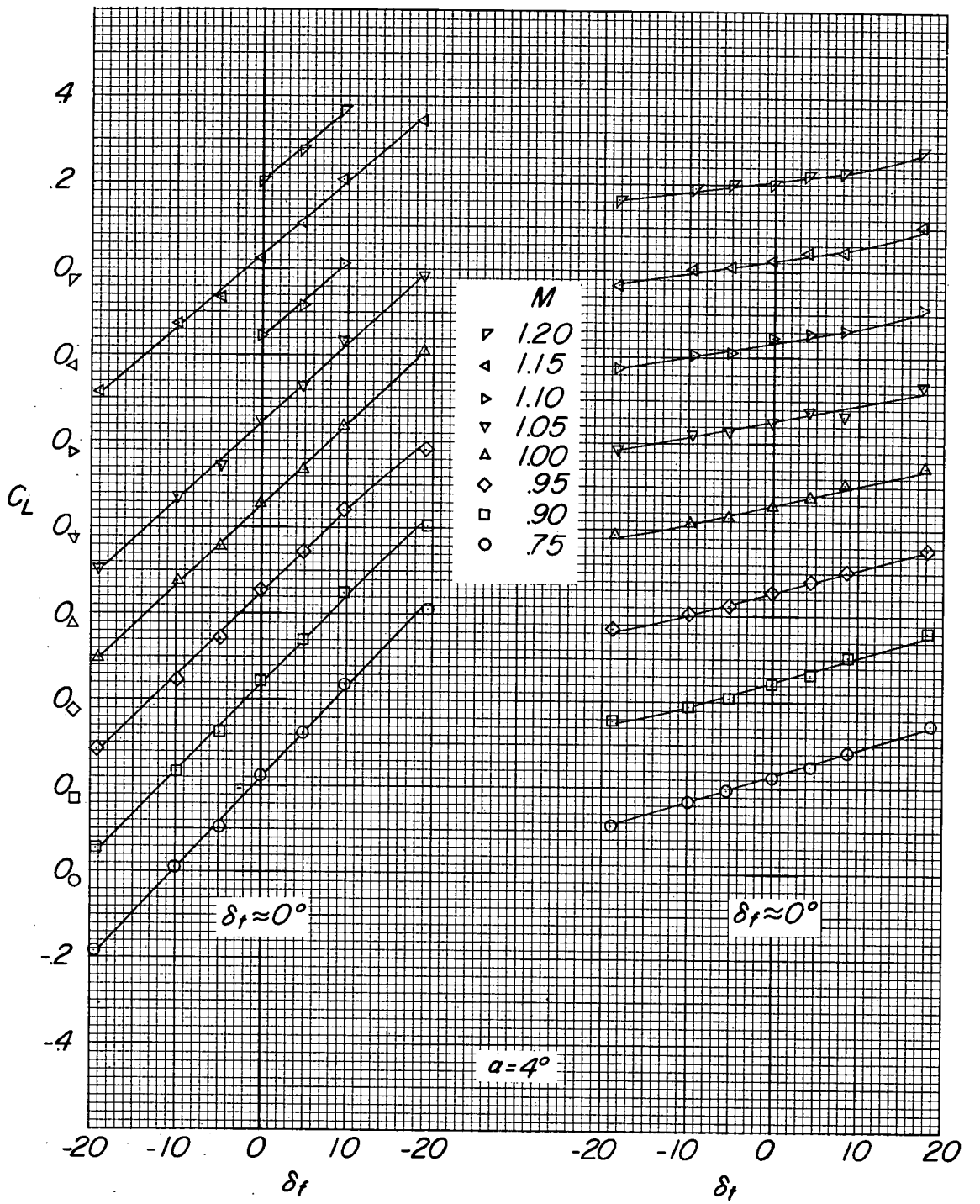

Figure 13.- Continued.

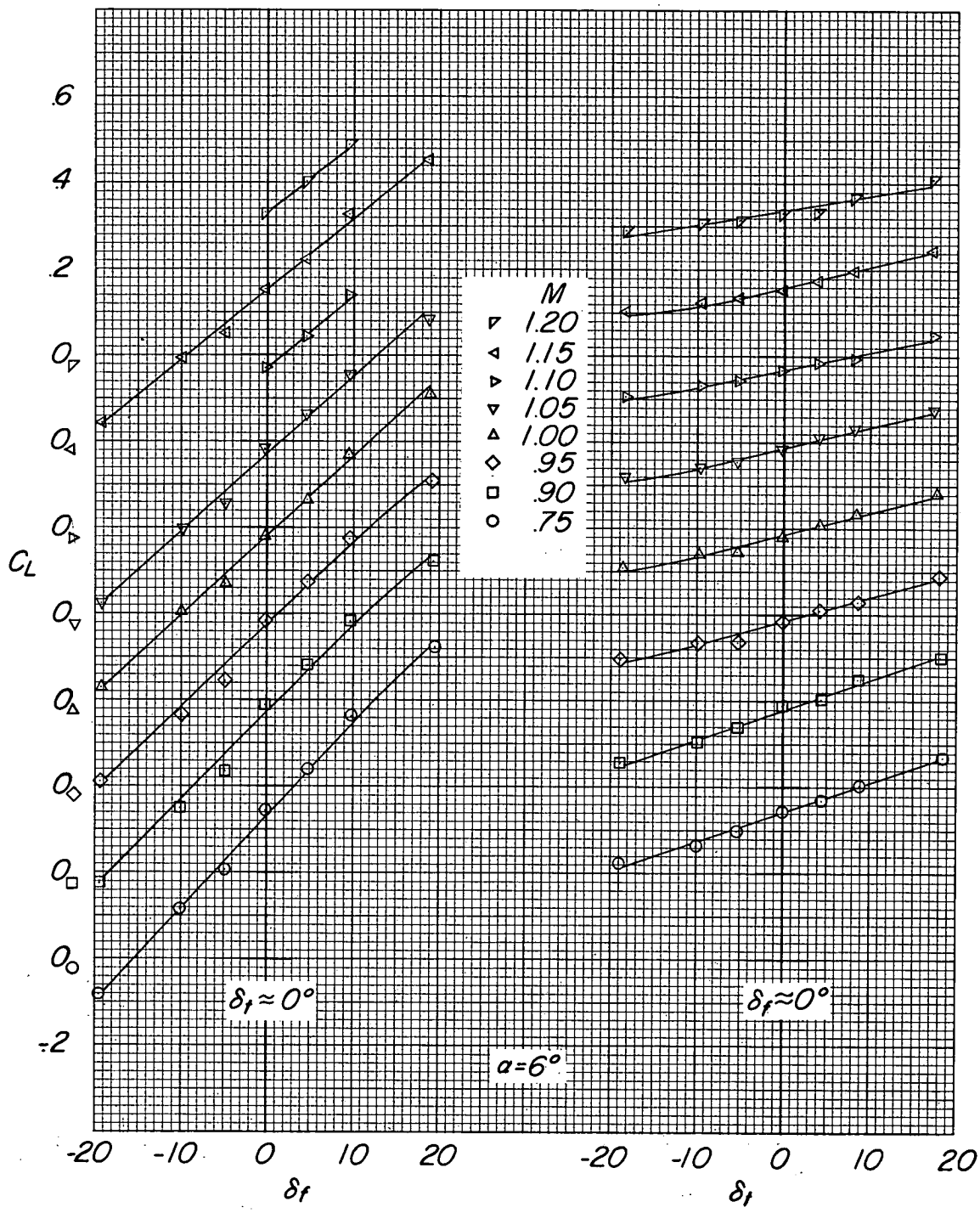

Figure 13.- Continued.

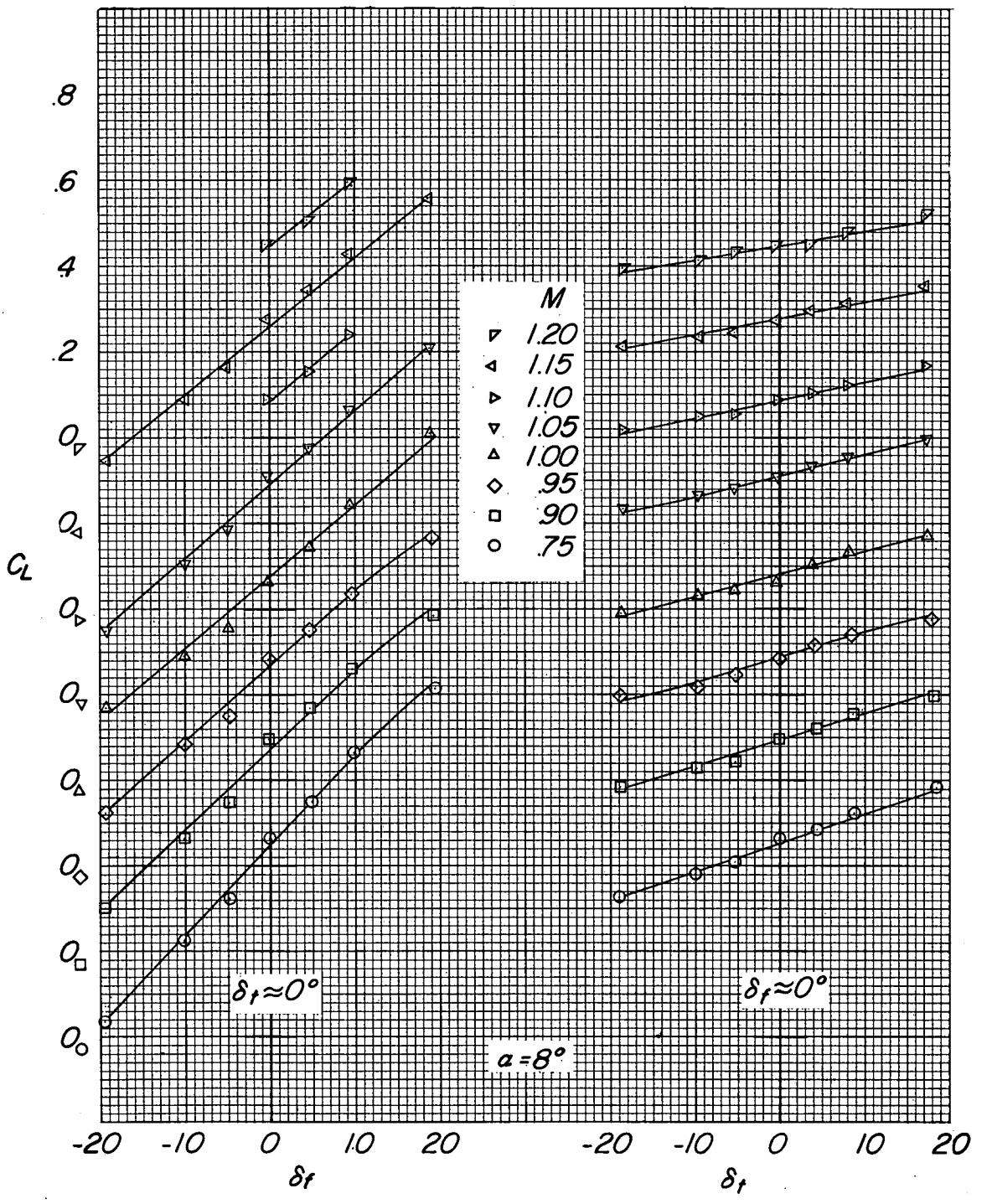

Figure 13.- Continued.

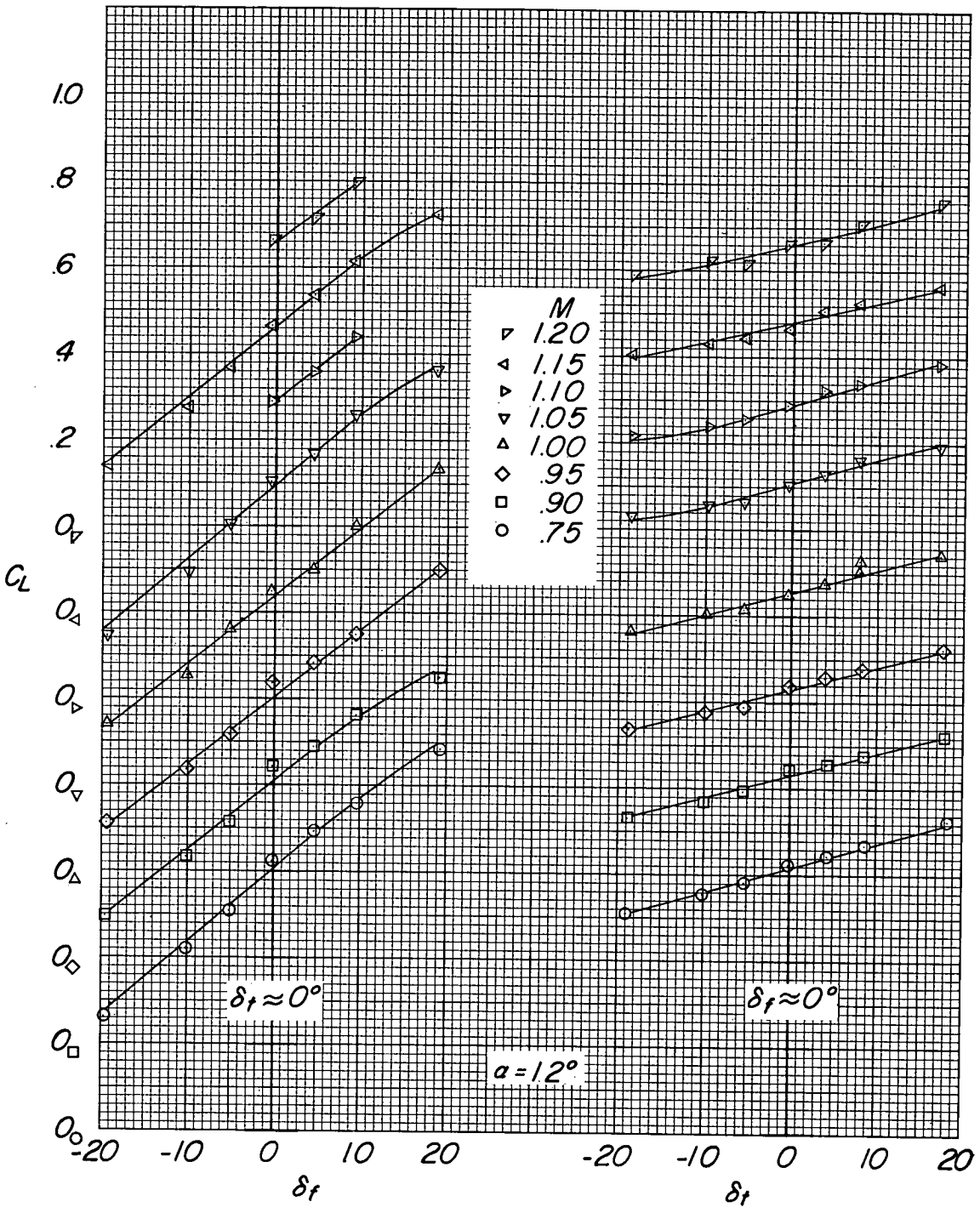

Figure 13.- Continued.

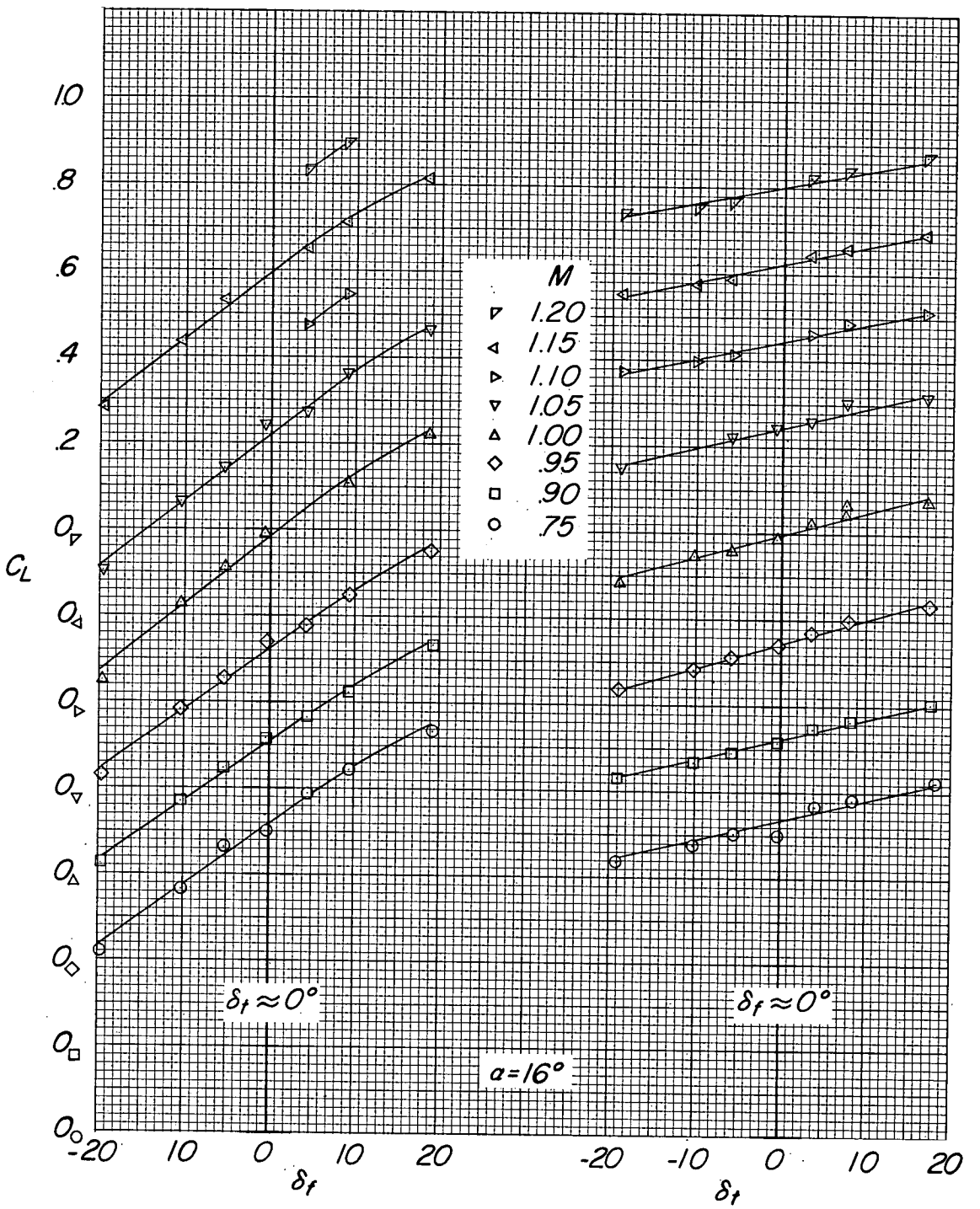

Figure 13.- Concluded.

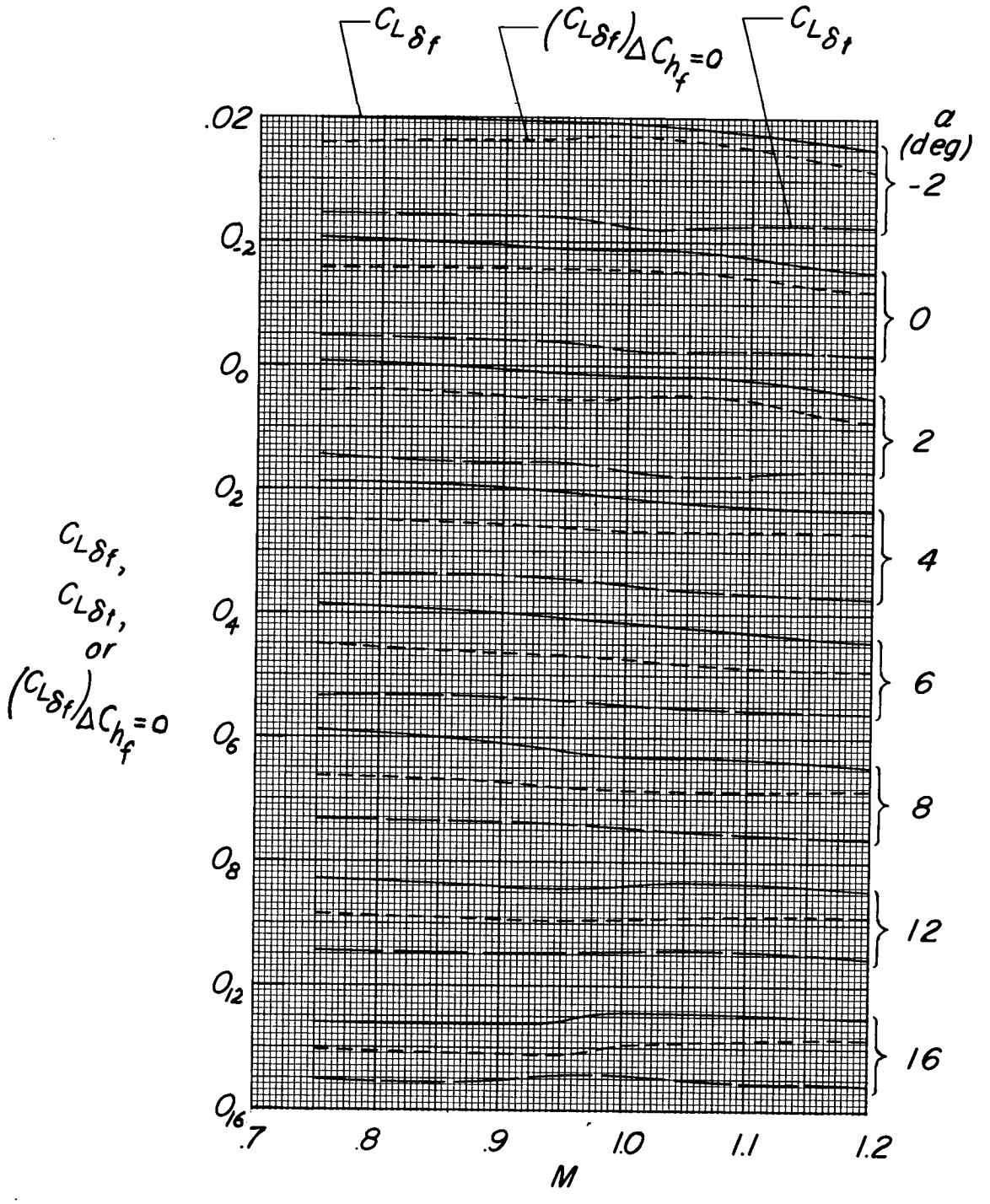

Figure 14.- Variation of tab lift parameter and balanced and unbalanced flap lift parameter with Mach number for various angles of attack.